Juvenile and Adult Fall Chinook and Chum Salmon Habitat Studies below Bonneville Dam on the Columbia River

Annual Report
2002 - 2003

DOE/BP-00004701-2

September 2004

This Document should be cited as follows:

Tiffan, Kenneth, Rodney Garland, Dennis Rondorf, Joseph Skalicky, "Juvenile and Adult Fall Chinook and Chum Salmon Habitat Studies below Bonneville Dam on the Columbia River", 2002 -2003 Annual Report, Project No. 199900301, 63 electronic pages, (BPA Report DOE/BP-00004701-2)

Bonneville Power Administration
P.O. Box 3621
Portland, OR 97208

This report was funded by the Bonneville Power Administration (BPA), U.S. Department of Energy, as part of BPA's program to protect, mitigate, and enhance fish and wildlife affected by the development and operation of hydroelectric facilities on the Columbia River and its tributaries. The views in this report are the author's and do not necessarily represent the views of BPA.

Annual Report 2002-2003

JUVENILE AND ADULT FALL CHINOOK AND CHUM SALMON HABITAT STUDIES BELOW BONNEVILLE DAM ON THE COLUMBIA RIVER

September 2004

USGS
science for a changing world

BONNEVILLE
POWER ADMINISTRATION

JUVENILE AND ADULT FALL CHINOOK AND CHUM SALMON HABITAT STUDIES BELOW BONNEVILLE DAM ON THE COLUMBIA RIVER

Annual Report 2002-2003

Prepared by:

Kenneth F. Tiffan

U.S. Geological Survey
Western Fisheries Research Center
Columbia River Research Laboratory
5501A Cook-Underwood Rd.
Cook, Washington 98605

Prepared for:

U.S. Department of Energy
Bonneville Power Administration
Environment, Fish and Wildlife Department
P.O. Box 3621
Portland, OR 97208-3621

Project Number 1999003

http://www.efw.bpa.gov/cgi-bin/FW/Publications.cgi

September 2004

Table of Contents

Table of Contents.....ii

Executive Summary.....iii

Acknowledgements.....iv

Chapter One:
Modeling subyearling fall Chinook salmon rearing habitat and dewatered areas below Bonneville Dam on the Columbia River.....1

Chapter Two:
Diel spawning behavior of chum salmon in the Columbia River.....41

Executive Summary

We investigated spatial and temporal changes in subyearling fall Chinook salmon rearing habitat and areas dewatered below Bonneville Dam on the Columbia River. We used two-dimensional hydrodynamic modeling to predict water velocity and depth data. By combining two-dimensional hydrodynamic modeling with a predictive model of subyearling rearing presence, we were able to illustrate spatiotemporal changes in subyearling rearing areas, areas dewatered by flow reductions, and percentage of dewatered locations that were initially subyearling rearing areas. By using a geographic information system, we located areas of persistent subyearling rearing and areas frequently dewatered at 1-h change intervals from 1 April through 31 May, 2003. We validated predicted water velocities and surface elevations using empirically collected water velocities and surface elevations. We beach seined to collect subyearlings at random locations within the study area to validate predictions of subyearling presence.

There was general agreement between empirically collected water velocities, water surface elevations, and subyearling presence, and modeled predictions of these measures. The average deviation between empirical and modeled water surface elevations was 0.1 m. The overall classification accuracy of predicted subyearling presence and absence was 80%.

We found an inverse relationship between Bonneville Dam discharge and hectares of subyearling rearing area. Temporally, subyearling rearing area decreased over the study period and large decreases in hourly discharge increased the hectares dewatered. The majority of subyearling rearing and dewatered areas occurred around Ives and Pierce islands. The hectares of pools disconnected from the river were maximized at discharges less than 6,760 m^3/s and greater than 9,750 m^3/s. Approximately 78% of all the hectares dewatered were initially subyearling rearing areas. Our study identified flow thresholds where pools occur and are known to strand and entrap fish. The findings presented in this study provide the information necessary for fisheries managers to develop strategies to minimize stranding and entrapment while optimizing rearing opportunities.

We investigated diel differences in chum salmon spawning behavior in the Columbia River in 2003. We used a dual-frequency identification sonar to quantify spawning behavior during both the day and night. Fourteen different pairs of chum salmon were observed continuously resulting in the collection of 79 h of daytime and 111 h of nighttime observation excluding crepuscular periods. We documented spawning events for 10 different pairs of chum salmon, of which three pairs spawned twice. Of the 13 observed spawning events, nine occurred during the night and four occurred during the day. Statistical analyses found no significant diel differences in female digging activity during nest construction, tail-crossing by courting males, and chase events initiated by female fish. Chase events made by males of day-spawning pairs occurred significantly more often at night, but we attributed this to one active male fish. Once chum salmon begin nest construction, visual cues are apparently not required for courtship, nest defense, and spawning. Our findings suggest that minimum daytime flows may be an inadequate strategy to restrict the distribution of chum salmon spawning, and diel flow fluctuations may disrupt the complex pre-spawning behavior that occurs both during the day and night.

Acknowledgments

We are grateful to the U.S. Army Corps of Engineers and the U.S. Geological Survey, Water Resource Discipline for sharing data vital for the completion of this study. Special thanks to Henry Franzoni of the Fish Passage Center for providing river data and programming assistance. We appreciate Dr. Peter Steffler and Dr. Terry Waddle's insights on the hydrodynamic model. We are especially thankful to my colleagues at the U.S. Geological Survey, Biological Resources Discipline, Columbia River Research Laboratory and the U.S. Fish and Wildlife Service, Columbia River Fisheries Program Office for help with data collection and advice. Thanks to the Washington and Oregon Departments of Fish and Wildlife for their help, support, and providing data. Finally, we wish to thank the Bonneville Power Administration for funding this work and Debbie Docherty for project oversight.

CHAPTER ONE

Modeling Subyearling Fall Chinook Salmon Rearing Habitat
and Dewatered Areas Below Bonneville Dam on the Columbia River

by

Rodney D. Garland, Kenneth F. Tiffan, and Dennis W. Rondorf
U.S. Geological Survey
Western Fisheries Research Center
Columbia River Research Laboratory
5501A Cook-Underwood Rd.
Cook, Washington 98605

Introduction

The Columbia River below Bonneville Dam supports a reproductive population of fall-run Chinook salmon near Ives and Pierce islands (Hymer 1997). This population is composed of two stocks. One is the Lower Columbia River fall Chinook salmon stock (also referred to as Tule), which is listed as "threatened" under the Endangered Species Act (NMFS 1999). The other is the upriver bright stock, the majority of which spawn 325 km upriver in the Hanford Reach of the Columbia River and is a relatively healthy population (Chapman 1943).

Juvenile fall Chinook salmon or "subyearlings" emerge from redds and rear below Bonneville Dam from approximately March to July (van der Naald et al. 2002). Subyearlings generally rear along shorelines in shallow, low-velocity areas (Dauble et al. 1989; Tiffan et al. 2002). Hourly fluctuations in discharge from Bonneville Dam can potentially change the amount and distribution of suitable rearing areas for subyearlings. Although subyearlings often show no directionality (upriver or downriver) in shoreline movements, Venditti et al. (1996, 1997) observed subyearlings moving downriver in greater numbers under high flows, which they attributed to changes in discharge. These fluctuations in discharge can potentially displace subyearlings from suitable habitats and cause them to move through unsuitable habitats and areas that contain predators and lower growth opportunity.

Rapid decreases in discharge can also cause high mortality in low-gradient areas by stranding fish on dewatered shorelines, or entrapping them in pools that become disconnected from the river (Wagner et al. 1999). Nugent et al. (2002) estimated that 125,000 subyearlings died due to stranding and entrapment in a 35.6-km section of the Hanford Reach (approximately a third of the reach). Waters can recede rapidly from near-shore rearing areas below dams due to powerpeaking, which is the fluctuation of river discharge to produce hydroelectric power (Figure 1).

Direct measurement of changes in subyearling rearing, stranding, and entrapment areas is difficult and expensive. We used a geographic information system (GIS)-based method for examining temporal changes in subyearling rearing areas, and shoreline dewatering and how these changes affect subyearlings. This approach has the potential for providing a practical method to assess a broad geographic scale and a dynamic environment, providing a more comprehensive examination of complex systems at a lower cost than more traditional methods. We used a combination of GIS, hydrodynamic modeling, and a predictive rearing model to investigate the effect of discharge changes on two factors: (1) total subyearling rearing area below Bonneville Dam and (2) areas subject to frequent dewatering. We hypothesized the: (1) amount of available subyearling rearing areas would be directly proportional to Bonneville Dam discharge, (2) amount of area dewatered below Bonneville Dam would be in direct proportion to the magnitude of the decrease in discharge, and (3) the probability dewatering suitable subyearling rearing habitat would be high following a decrease in Bonneville Dam discharge. We tested these hypotheses using a case study during the peak subyearling rearing period below Bonneville Dam of April and May in 2003 (van der Naald et al. 2002; van der Naald et al. 2003).

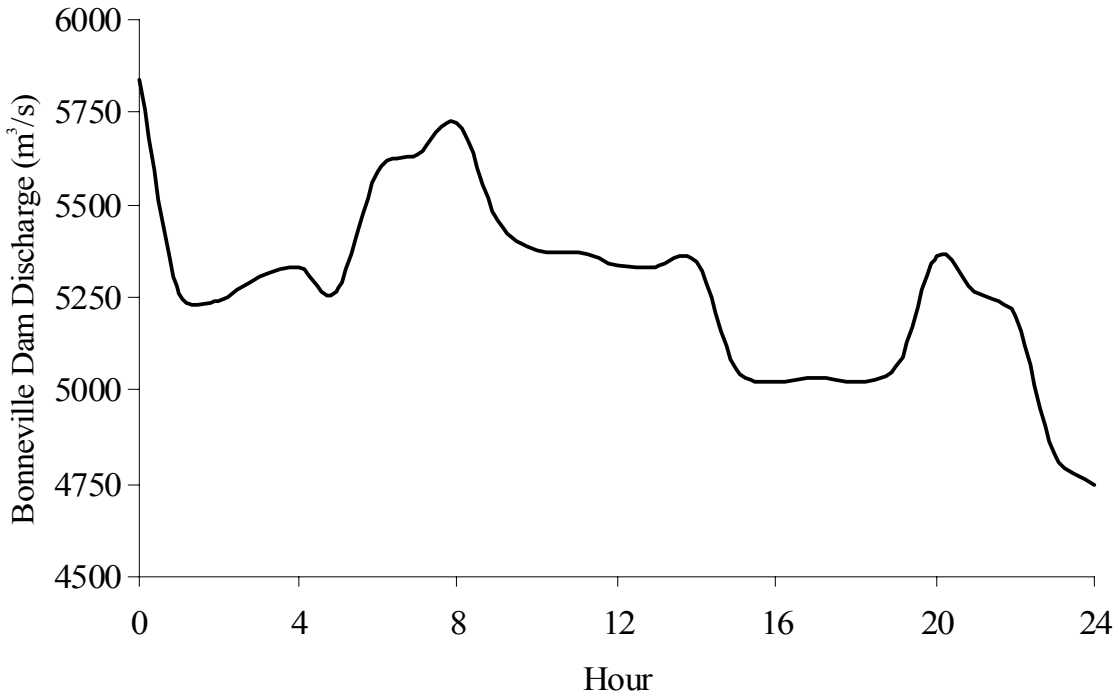

Figure 1. – An example of hourly discharge fluctuations originating from Bonneville Dam on 3 April 2003. Data were collected by the COE and provided by Henry Franzoni (Fish Passage Center, Portland, OR, Unpublished Data).

Study Area

Our study area was located on the Columbia River, 3.5 km below Bonneville Dam between river kilometers (Rkm) 215.5 and 231.5, as measured from the mouth of the Columbia River (Figure 2). This area contains three islands: Ives, Pierce, and Skamania. The northern shoreline and all islands are in Skamania County, Washington and the southern shoreline is in Multnomah County, Oregon. We selected this river section for its complex channel morphology, location below a major dam, the presence of an important spawning population of fall Chinook salmon, and the availability of base bathymetry and substrate surface information.

We divided the study area into seven study sections (Figure 2) to facilitate our comparison of four fluvial features: (1) islands, (2) main-channel reach, (3) upper reach, and (4) lower reach. Section 1 includes Ives Island and the Washington shoreline north of the island. Section 2 includes Pierce Island and the Washington shoreline north of the island. Section 3 includes the Washington shoreline downriver from Pierce Island to a point halfway from Pierce Island to the lower end of Skamania Island. Section 4 includes the Washington shoreline downriver from section three to the downriver end of the study area just past Skamania Island. Section 5 includes the Oregon shoreline, from just above Ives Island to a point halfway downriver to the lower end of the study area. Section 6 includes the Oregon shoreline downriver from section five to the downriver end of the study area. Section 7 delineates Skamania Island, excluding any main river shoreline areas. The island reach included study sections 1, 2, and 7, while the main-channel reach included study sections 3, 4, 5, and 6. The upper reach included study sections 1, 2, 3, and 5, while the lower reach included study sections 4, 6, and 7.

The Bonneville study area is subject to both hydroelectric control of discharges and tidal fluctuations. Hydroelectric development has reduced peak annual discharges by an average of over 40% and peak river stages (water surface elevations, or WSE) by 0.5-2.0 m during the spring and summer migration of juvenile salmonids (Bottom et al. 2001). Cyclical oscillations in WSE caused by ocean tides and backwater effects from the Willamette River (Rkm 162), changes the WSEs throughout the reach (Figure 3). Tidal stage decreases in an inland direction toward Bonneville Dam. There is little information on, or analysis of, tidal or Willamette River backwater influences up to Bonneville Dam. However, backwater effects do extend to the face of Bonneville Dam. These natural and anthropogenic modifications in WSE and discharge patterns create a dynamic process of spatial and temporal change in water depths and velocities throughout the Bonneville study area.

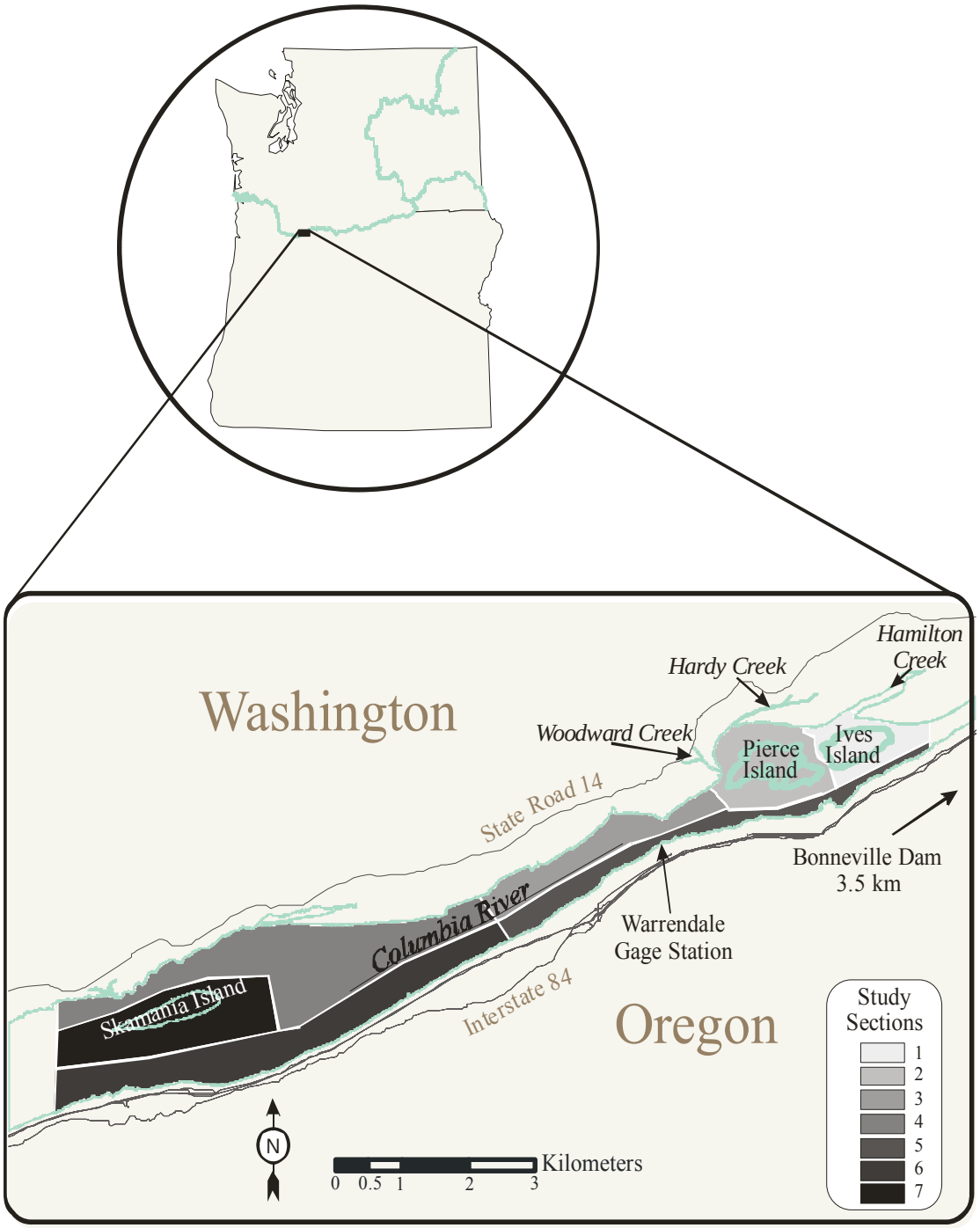

Figure 2. – The location of the Bonneville study area on the Columbia River in Oregon and Washington, showing the areas that comprised the seven study sections.

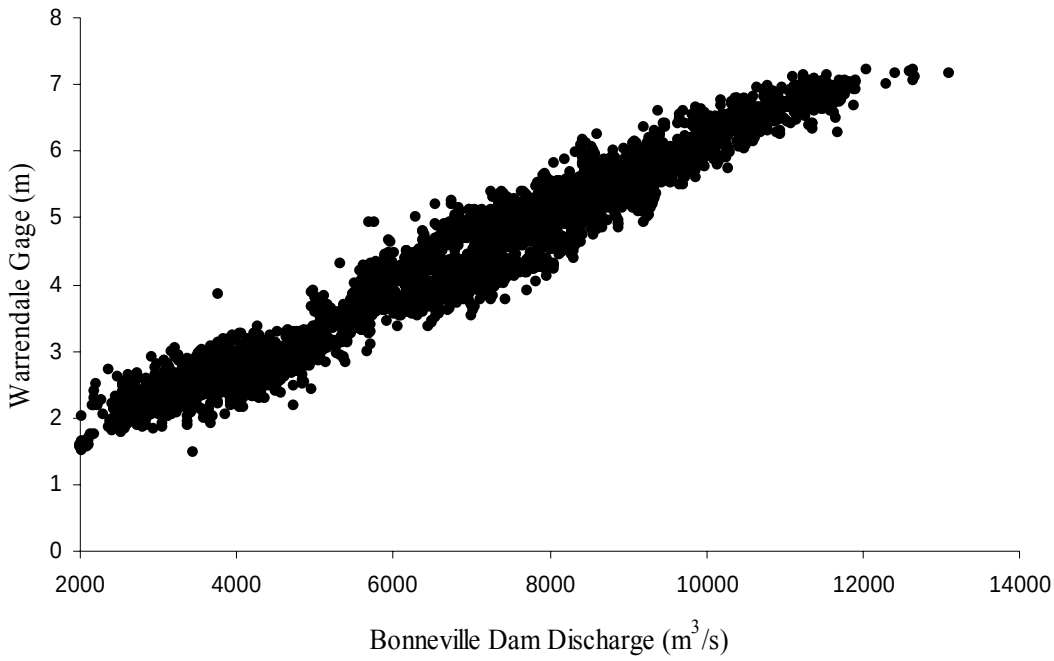

Figure 3. – Variations in WSE at the Warrendale gage station compared to Bonneville Dam discharge for the years of 1981 to 1986, 2001, and 2002. Bonneville Dam discharge data were collected by the COE and provided by Henry Franzoni (Fish Passage Center, Portland, OR, Unpublished Data) and Warrendale data provided by Suzanne Miller (U.S. Geological Survey, Portland, OR, Unpublished Data).

Methods and Analysis

Riverbed Bathymetry

Detailed riverbed bathymetry was required for two-dimensional hydrodynamic modeling, which we used to estimate water velocities and depths in our study area over a range of flows. We created a digital elevation model (DEM) that incorporated riverbed bathymetry and surrounding topography from five existing data sources (Table 1). The first source included Bonneville Power Administration (BPA) elevation data for Ives and Pierce islands and the Washington shoreline north of these islands collected in 1999 (John Moore, BPA, Portland, OR, unpublished data). The data originated from 0.3-m contour topographic data using photogrammetry. Aerial adjustments and data collection used a Zeiss P1 analytical stereo plotter. The second data source included U.S. Army Corps of Engineers (COE) depth soundings collected along transects in the Bonneville study area in 1999 (Ken Kleczynski, COE, Portland, OR, unpublished data). These data were collected using a differential correcting geographic positioning system (DGPS) that provides sub-meter accuracy for the horizontal positions. We obtained above-water elevation data for the Oregon and Washington shorelines from U.S. Geological Survey (USGS) 7.5-minute (10x10 m) DEM data. The fourth and fifth datasets included total station and depth sounding data collected by the USGS and U.S. Fish and Wildlife Service (USFWS) in 2000 and 2001 (Garland et al. 2003).

For areas with missing or sparse data, we collected elevation points using a depth sounding system coupled with a DPGS. Depth data were converted to elevations by subtracting depths from WSE data measured from a vertical ground control with an electronic total station. The final DEM of the Bonneville study area was created by combining all datasets. We checked the final DEM for errors using a triangulated irregular network (TIN) within a GIS, and removed error points based on the smoothness of the topography between all points (Basu and Malhotra 2002).

Substrate Roughness

Two-dimensional hydrodynamic modeling requires information on substrate surface roughness. A map of dominant surface substrates was created for the areas between Rkm 226.9 and 231.5 from a previous study (Garland et al. 2003). This substrate map delineated the spatial extent of textural patches (i.e., grain-size facies) of dominant substrates (Buffington and Montgomery 1999) using a visual classification method modified from Bovee and Scott (2002; Table 2) for 1x1 m areas in dry land and waters <0.5 m deep. For waters deeper than 0.5 m, Garland et al. (2003) used a boat and underwater video camera to classify substrates. We used a DGPS to determine the geographic positions at each location. Delineation of textural patches used an approach similar to the facies-stratified random approach described in (Buffington and Montgomery 1999). A total of 4,718 substrate data points were collected to delineate textural patches. We generated the final map using thiessen polygons, adjusted manually based on aerial photographs and field notes.

Table 1. – Sources, horizontal resolutions, and vertical resolutions of existing data used to create the DEM of the Bonneville study area.

Data Source	Horizontal Resolution (m)	Vertical Resolution (m)
BPA, Photogrammetry, 1999	0.06	0.15
COE, Sounder Transects, 1999	< 1	0.3
USGS, DEM	Varies	Varies
USGS, USFWS, Total Station Surveys, 2000-2001	0.15	0.1
USGS, USFWS, Sounder Transects, 2000-2001	< 1	0.3

Table 2. – Particle sizes, and descriptions used to classify substrates.

Particle Size (mm)	Description
≤4	Sand/Silt
4-75	Gravel
75-150	Small Cobble
150-300	Large Cobble
>300	Boulder
NA	Bedrock

We assigned substrate roughness values to delineate textural patches from a grain-size distribution study (Garland et al. 2003), which was determined using a grain-count method (Wolman 1954; Kondolf 1997). We sampled random locations within textural patches along 18, 30.5-m transects that followed a random compass direction. Measurements of 100 grains along the intermediate axis of each grain at 0.3-m intervals along each transect were used to determine the grain size (mm). For substrates smaller than 4 mm, we used an assignment of "< 4 mm" (Kondolf 1997). Grain size measurements provided the D84 (the size below which 84% of the samples are finer) values for each transect.

Hydrodynamic Modeling

We used the River2D two-dimensional hydrodynamic model (Ghanem et al. 1996) to estimate depth-averaged water velocities throughout the Bonneville study area at 1-h intervals for the months of April and May, 2003. This model solves shallow-water flow equations by applying a two-dimensional finite-element method. Two-dimensional hydrodynamic model inputs included riverbed topography with geographic position and substrate roughness height as well as inflow discharges and the WSE for the downriver end of the modeled area. The two-dimensional hydrodynamic model uses substrate roughness values, which we derived from the D84 textural patch study. We expressed the D84 data for each textural patch in meters and doubled the resultant values to estimate substrate roughness (P. Steffler, University of Alberta, Edmonton, personal communication). In areas where substrate roughness data were lacking, we assigned a uniform value of 0.1-m, as determined during model calibration. Modeled velocities are typically insensitive to substrate roughness except in shallow waters (Ghanem et al. 1996).

We used position, elevation, and substrate roughness data to create an initial triangulated irregular mesh for use in the hydrodynamic model. We generated a computational mesh at a uniform node spacing of 25 m from the empirical DEM. We used constant inflow discharge for the Columbia River and Hamilton Creek, and downriver WSE to model steady-state flows. Steady-state conditions exist when the upriver and downriver discharge and WSE are constant, resulting in a stable flow (Graf 1998).

After achieving steady-state conditions, we regenerated the computational mesh to increase shallow-water node densities while retaining a lower node density in deep water. We did this using the same methods described above, except that the River2D program assigned depths to each computational node during the initial uniform modeling. These depths allowed us to add more nodes in shallow-water areas. Rerunning the two-dimensional hydrodynamic model to steady-state using numerous discharges and WSE values, adding nodes in shallow-water areas, and repeating the mesh generation process was used to create the final computational mesh. The highest node resolution in the final computational mesh was approximately 4 to 5 meters. Because the River2D model can only accurately estimate bed features of horizontal size less than ten times the water depth (Steffler and Blackburn 2002), the 4 to 5 meter resolution approximates the maximum density given the size of the study area.

Modeling proceeded by assigning inflow discharges from Bonneville Dam, Hamilton Creek at a location 250 m upstream of its mouth, and assigning a WSE to the downstream end of the Bonneville study area. Hourly discharge data for the Columbia River originated from the COE at Bonneville Dam (Fish Passage Center, Portland, OR, unpublished data) and WSE data was obtained from the USGS (USGS, Portland, OR, unpublished data). We used a single discharge value of 5-m^3/s for Hamilton Creek discharge for the entire modeling period. This value originated from empirical discharge measurements taken in the spring of 2001. No other discharge information for Hamilton Creek was available, nor was there any discharge data available from the smaller tributaries in the area.

We estimated downriver WSEs using data from the USGS Warrendale Oregon gage station (Gage number 14128910; discontinued after 2002), which was located 10 km above the downriver end of the Bonneville study area, because there was no gage station at the downriver end of our study area. To correct for this locational difference, we derived a multiple regression equation to predict WSE at Warrendale using WSE data from the Vancouver Washington gage station (Gage number 14144700) and Columbia River discharges at Bonneville Dam as the independent variables. The Vancouver gage station is located 54 km downriver of the Warrendale gage station. WSE at the Warrendale gage station was the dependent variable. We used hourly data from 2001 and 2002, a period when both gages were operational. We used the multiple regression equation to estimate hourly Warrendale gage station WSEs for the study period. A value of 0.11 m was subtracted from the multiple regression estimates of the WSE at Warrendale to determine the WSE for the downriver boundary of the Bonneville study area. This was determined by making a series of coarse-scale hydrodynamic model runs at various flows and Vancouver gage WSE values for the area from the Vancouver gage station to the upstream end of the Bonneville study area.

We calibrated our WSE data using 20 empirical WSE values from the Warrendale gage station and WSE points collected using an electronic total station around Ives Island. We identified model inaccuracies by comparing measured WSE values to WSE values generated by the two-dimensional hydrodynamic model. Initially, the largest observed inaccuracy was 0.37 m. Based on these differences, we changed the substrate roughness values used by the two-dimensional hydrodynamic model for all nodes by adding or subtracting an appropriate roughness value, and increasing the density of computational nodes in specific locations to calibrate the model. We ran the model and compared the empirical and modeled WSE values until the empirical and modeled WSE values were within 0.2 m, which is lower than the bathymetries accuracy of 0.3 m (Table 1). We repeated this process until all WSE point locations had differences less than 0.2 m.

We validated modeled water velocities using empirical data collected with an acoustic Doppler current profiler (ADCP), a DGPS, and 61 empirical WSE values that were not used for model calibration. An ADCP measures water velocity by calculating the Doppler-shift of acoustic echoes returned from small, suspended materials in the water column and then converts these echoes into a water velocity. For depths greater than 1-m, velocity measurements were made along cross sections placed perpendicular to the current at randomly designated locations. A greater concentration of transects were placed in the side channels of Ives and Pierce islands than in the main channel of the Columbia River. ADCP

cross-sectional profiles are divided into a grid based on horizontal distance and depth. A DGPS was used to georeferenced the midpoint of each horizontal segment. For the Columbia River transects each grid cell, or "bin", measured 2 m long by 0.25 m deep. In contrast, the shallower side-channel transect bins measured 1 m long by 0.1 m deep. We used the root mean square of water velocities for each vertical bin array to determine the total water column velocity for each horizontal section. A wading rod, current meter, and DGPS were used to collect velocity data in areas < 1 m deep. If depths were < 0.76 m, the 60%-depth velocities were used, otherwise velocities were averaged for 20% and 80% water depths if the water was ≥ 0.76-m deep (Orth 1983).

To capture natural variations in water velocities caused by water turbulence and natural pulsing of flows, we collected 3-10 replicate ADCP profiles at 25 cross sections. Each cross-sectional profile was divided into 10-m long sections and the average and standard deviation of the velocity for each section was calculated from the replicate data. We determined the modeled water velocity at the time of each ADCP profile was collected. We graphically compared modeled and empirical water velocity data. We also used Spearman's correlation coefficient to determine the correlation between the empirical and modeled water velocity data. Statistical significance was assumed at $P \leq 0.05$. We also used the root mean squared error (RMSE) and the average systematic error (MSE_S) values to assess differences between empirical and modeled data (Willmott 1981). We used RMSE to determine the error between observed and predicted water velocity, with a low RMSE indicating low error in the units of measure of the data collected. MSE_S is a measure of overall systematic error, with low values indicting a better overall agreement between observed and predicted values.

The two-dimensional hydrodynamic model was validated using empirically-measured WSE values. We estimated WSE for six dates using the two-dimensional hydrodynamic model. Sixty-one empirical WSEs were collected on these dates using an electronic total station (Figure 4). The differences between empirical WSE measures and simulated WSE values were used to identify locations with a poor agreement. We also used the RMSE to assess differences between the empirical and modeled WSE data for each of the six dates (Willmott 1981). We did not use MSE_S to assess differences in WSE data because this measure uses the slope and intercept from the relationship between predicted and observed WSE. We did not have enough data points from each date to assess these measures.

After computational mesh calibration and validation runs were completed, we conducted model simulations for each hourly time step for the April-May study period, which resulted in 1,464 simulations. Because the minimum temporal resolution of our flow data was 1 h, we modeled flow for each 1-h time step as steady-state. Open-channel flows are rarely steady-state in nature, however, for relatively short time intervals, the flow can be assumed steady (Graf 1998). As each hourly flow was modeled using an instantaneous measurement of discharge and WSE, we assumed that each 1-h instantaneous model output approximated steady-state. Each of the 1,464 model simulations generated a two-dimensional file of water depths and water velocities.

Each water velocity and water depth dataset derived from hourly two-dimensional hydrodynamic model outputs were used to generate a grid in a GIS. Node locations were

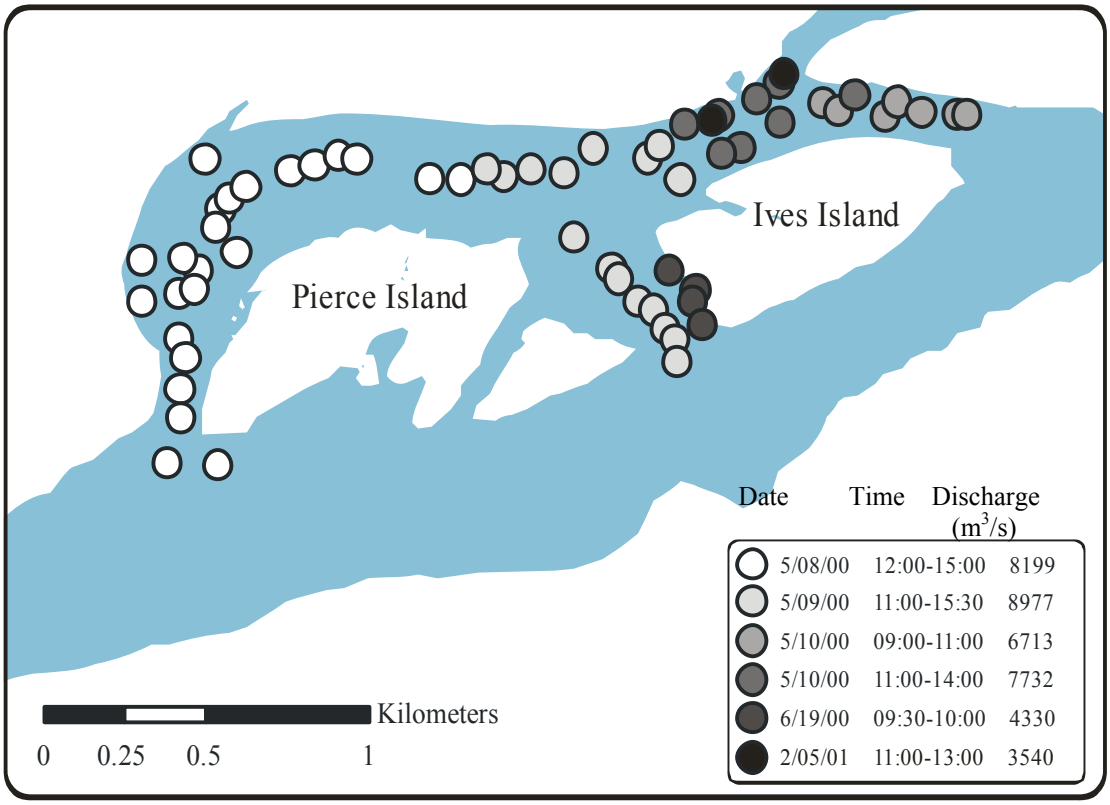

Figure 4. – Locations of empirical WSE sampling points as well as the date and time range of data collection and the average discharge during sampling.

interpolated into 4-m resolution (16 $m^{2)}$ grid cells using a linear method. In addition, the original DEM of the Bonneville study area was used to create a 4-m resolution grid of percent slope. Water velocity, water depth, and the percent slope grids provided the base information required for using an existing subyearling rearing presence model.

Analysis of Presence of Rearing Subyearlings

We used a statistical model and habitat parameters derived from a previous study to predict the presence of rearing subyearlings at different Bonneville Dam discharges and downriver WSEs. Tiffan et al. (2002) created a logistic regression model of subyearling rearing presence and absence in the Hanford Reach of the Columbia River using slope and water velocity. Their final multivariate model can be expressed as:

$$g(x) = -3.19 + 2.23V_1 + 2.45V_2 + 1.96V_3 + 2.66S_1 + 2.42S_2 + 2.28S_3 + 1.04S_4,$$

where $V_{1\text{-}3}$ represents different categories of water velocity, and $S_{1\text{-}4}$ represent different categories of slope (Table 3). From this equation a probability P_i of subyearling presence in i shoreline habitat cells given the habitat characteristics of each cell was calculated. Expression of the probability P_i uses the equation

$$P_i = \frac{e^{g(x)}}{1 + e^{g(x)}},$$

where g(x) is the linear combination of parameter estimates obtained from the logistic regression. These equations provided the foundation for a grid-based assignment of the probability of presence of rearing subyearlings in habitat cells near the shoreline. In addition, Tiffan et al. (2002) observed non-use of habitats occur where water velocities were greater than 0.71-m/s and water depths were greater than 1.5-m. We applied the same habitat parameters for this study, and used a probability level of 0.8 to define suitable habitat areas. This high probability level made estimates of suitable rearing areas conservative. These equations and thresholds were used to create rearing area grids from each of the 1,464 hydrodynamic model simulations, and rearing areas were assigned a value of 1 if they were suitable or 0 if they were not.

Table 3. – Summary of the logistic regression models variable categories for velocity and slope from (Tiffan et al. 2002).

Variable	Variable Category
Velocity (V_1)	0.0 – 0.1 m/s
Velocity (V_2)	0.1 – 0.2 m/s
Velocity (V_3)	0.2 – 0.4 m/s
Slope (S_1)	0 – 10 %
Slope (S_2)	10 – 20 %
Slope (S_3)	20 – 30 %
Slope (S_4)	30 – 40 %

The final step of modeling rearing areas was to remove simulated pool areas that were disconnected from the river. We did this by converting the water depth grids for each 1-h increment to land/water binary maps where land was assigned a value of 0 and water a value of 1. By converting these grids to polygon coverages and deleting the main river polygon (any areas greater than 500 hectares), only disconnected pools remained in the final grid. The areas of these pools were then summed to determine the hectares of disconnected areas. We then converted the binary rearing area grids into polygon coverages and intersected these with the disconnected pool polygons. Finally, the results from these operations were subtracted from the overall sums of rearing hectares so that the disconnected pool areas were not represented as rearing areas.

We collected empirical subyearling presence and absence data with a beach seine from 1 April to 15 April and 6 May to 20 May, 2003 to validate the rearing model results. Each sample occurred only within the Bonneville study area. During the first sampling period, beach seine locations were randomly determined *a priori* within a GIS. We used a DGPS to navigate to each sample site and sampled the area with a beach seine set 30.4-m parallel to the shoreline and approximately 7.6-m offshore, to sample a total area of 231-m^2. However, only sites with smooth substrates, low water velocities, and a lack of obstructions such as stumps, that may snag the net can be sampled effectively with a beach seine. When we were unable to seine at a random location, we sampled a site near the random location. During our second sampling period, we resampled each beach seine location from the first period, except when conditions did not make seining possible. In these situations, we seined locations as near as possible to the original site. Captured fish were sorted by species, counted, and a DGPS was used to mark the location of each beach seine site. We measured ten subyearlings from each seine haul to the nearest 1-mm. Subyearling catch results and rearing models results for the seined locations were compared using an accuracy assessment matrix of presence and absence (Lillesand and Kiefer 2000). We used the nonparametric Spearman's correlation coefficient to determine if an association existed between the predicted hectares of modeled rearing area and Bonneville Dam discharge and between modeled rearing hectares and WSE.

Because the Bonneville Reach was morphologically complex, we partitioned the study area to examine differences in rearing habitat at a smaller spatial scale. We examined differences between the upper and lower reaches, and between the island and main-channel reaches using rearing areas (ha) for each 1-h grid and standardized them by the length of shoreline. We standardized rearing areas using grids of water depth for each 1-h increment to create land/water binary grids where land equaled 0 and water equaled 1. This grid was then converted to a line coverage within a GIS. We intersected the line coverage with a polygon coverage of the reaches, creating line coverages with information on the length of the shorelines (km) for each reach and every 1-h time increment. We used the methods for adjustment of rearing area and from estimating shoreline length as described above to calculate the kilometers of disconnected pool shorelines. We subtracted the length of pool shorelines from the estimated total shoreline length to derive the final shoreline length. We standardized the final data set by dividing the total hectares of subyearling rearing areas by the length of shoreline for each reach created. We used the Mann-Whitney test to determine if there was a significant difference in the amount of rearing hectares/kilometer between the upper and lower, and between the island and main-channel reaches.

Lastly, we identified locations that were consistently available for subyearling rearing for all the hours modeled during the study period using a rearing persistence grid. Generating the rearing persistence grid required addition of all the hourly binary rearing grids using map algebra (DeMers 2002). Rearing areas assigned high numeric values for persistence were those that were most persistent over the season. We used the final persistence grid to convert the numeric occurrences of rearing areas into a percent rearing persistence grid. We calculated percent persistence by dividing the numeric persistence grid by the number of hourly events (1,464) and multiplying the resultant quotient by 100. The final subyearling percent rearing persistence grid showed locations that were consistently suitable for subyearling rearing during the study period.

Dewatered Area Analysis

We identified and quantified areas dewatered during periods of decreasing discharge and WSE using the binary water/land grids created in the rearing analysis. Using the "less than" relational operator (DeMers 2002), grid cells changing from 1 (water) to 0 (land) from the hour-one to hour-two grids were used to create a new grid where a value of 1 equated to "dewatered" and 0 equated to "not dewatered". This process was repeated for successive 1-h time change intervals to create the grids of dewatering events.

We used Pearson's correlation coefficient and linear regression to investigate the relationship between dewatered area, Columbia River discharge, and WSE for the entire Bonneville study area. Initial analysis indicted that the distribution of residuals was random, showing no autocorrelation or heteroscedastic trends. We began by summing the total hectares of dewatered areas individually for each dewatering event for the entire Bonneville study area and then separately for the islands, main-channel, upper, and lower reaches. These served as the dependent variables for analysis. We then calculated the 1-h change in Columbia River discharge (ΔQ), and the corresponding 1-h change in downriver WSE (ΔW). These served as the independent variables for analysis. Excluding dewatering data increments where the total hectares dewatered were less than 0.5 hectares was necessary to remove periods with no dewatering or with small grid and two-dimensional hydrodynamic modeling errors.

We used a dewatering occurrence grid similar to the rearing persistence grid to identify areas with numerous dewatering events during the entire study period. Generating the dewatering occurrence grid required summing all binary dewatering grids using map algebra. Locations with high numeric values are those at high risk for dewatering over numerous 1-h periods. The final dewatering occurrence grid was created by converting the numeric dewatering occurrences into percent occurrence. We calculated the percent occurrence by dividing the numeric occurrence grid by the number of 1-h change events (1,463) and multiplying the resultant quotient by 100. The final dewatering occurrence grid was used to identify locations that were frequently dewatered during the study period.

Finally, we determined the amount of dewatered area corresponding to areas predicted to be subyearling rearing areas. This procedure required the creation of new grids by adding

each dewatered grid to the subyearling rearing grid corresponding to the initial hour of a dewatering event (hour one), where a cell coded as 2 equated to an area that was both dewatered and initially good for subyearling rearing. The logic behind this approach was that subyearlings in shoreline locations at hour 1 would have to move out of area if the area was converted to land at hour 2. Calculation of the percentage of dewatered area that was initially suitable for subyearling rearing used the total hectares of dewatered area, divided by the hectares that were both dewatered and were initially suitable for subyearling rearing, and multiplying the quotient by 100. Finally, we calculated the mean and standard deviation of the calculated percentage for all time change periods.

Results

Two-dimensional hydrodynamic modeling coupled with a subyearling rearing model was a useful tool in predicting the location of rearing areas over a range of flows. A total of 1,464 Bonneville Dam hourly discharges were modeled and predictions of subyearling rearing areas were made for each discharge (Figure 5). We successfully quantified the influence of corresponding changes in discharge on changes in subyearling rearing areas and areas dewatered. However, determining WSE was a critical component for two-dimensional hydrodynamic modeling.

Our multiple regression analysis for determining Warrendale gage WSE values showed a strong relationship between Warrendale WSE, Vancouver WSE, and Bonneville Dam discharge values. Graphs of the regression residuals showed no autocorrelation or heteroscedastic trends. Bivariate linear regressions between the Warrendale gage WSE and each predictor variable resulted in an r^2 of 0.89 for Bonneville Dam discharge and an r^2 of 0.82 for Vancouver gage WSE. Expression of the final multivariate model was

$$W = 0.756 + 0.584V + 0.0003199B$$

where W represents predicted Warrendale WSE (m), V represents Vancouver WSE (m), and B represents Bonneville Dam discharge (m^3/s). The R^2 for this model was 0.96 and significant ($P < 0.000$).

Water velocities predicted by the two-dimensional hydrodynamic model agreed well with the empirical measures of water velocity. Modeled and empirical water velocities were significantly correlated ($P < 0.05$) for all of the 25 transect locations. The one exception was for a single transect located just downstream of Hamilton Creek (Figure 6; $P = 0.20$). The largest RMSE was 0.93 for the farthest upriver main-channel transect (Figure 6). The transect just downstream of Hamilton Creek had the next largest RMSE (0.37). The transect just downstream of Hamilton Creek had the largest MSE_S (0.1), and all others were >0.05. In areas with simple channel forms, modeled water velocities agreed well with the empirical data. At other locations with more complex bathymetry and flow patterns, water velocities diverged from the empirical data (Figure 6).

Empirical and modeled WSEs agreed closely with the greatest variation being less than the highest estimated potential error of 0.3 m in the topographic information. Fourteen

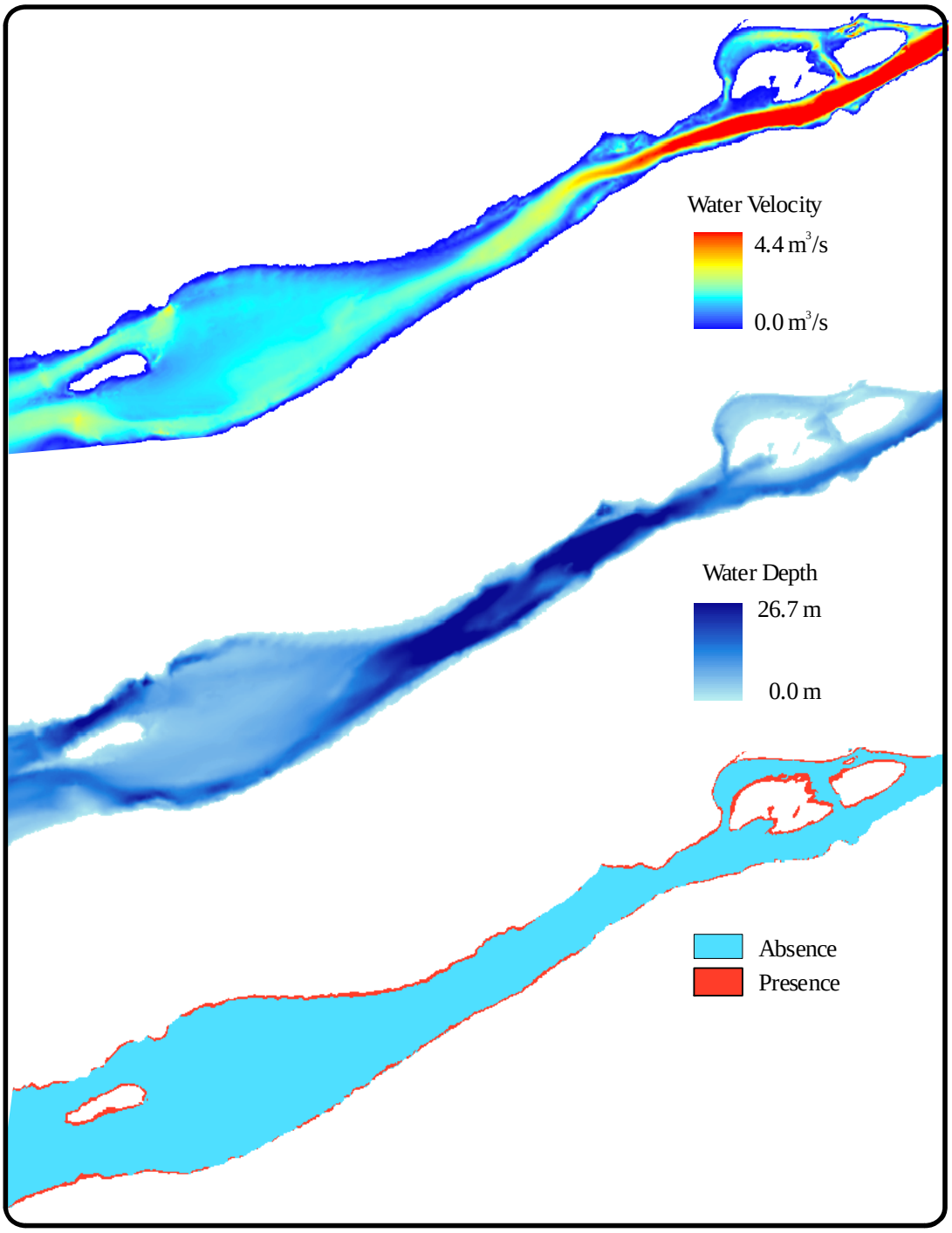

Figure 5. – Examples of water velocity, water depth, and rearing presence grids for the Bonneville study area.

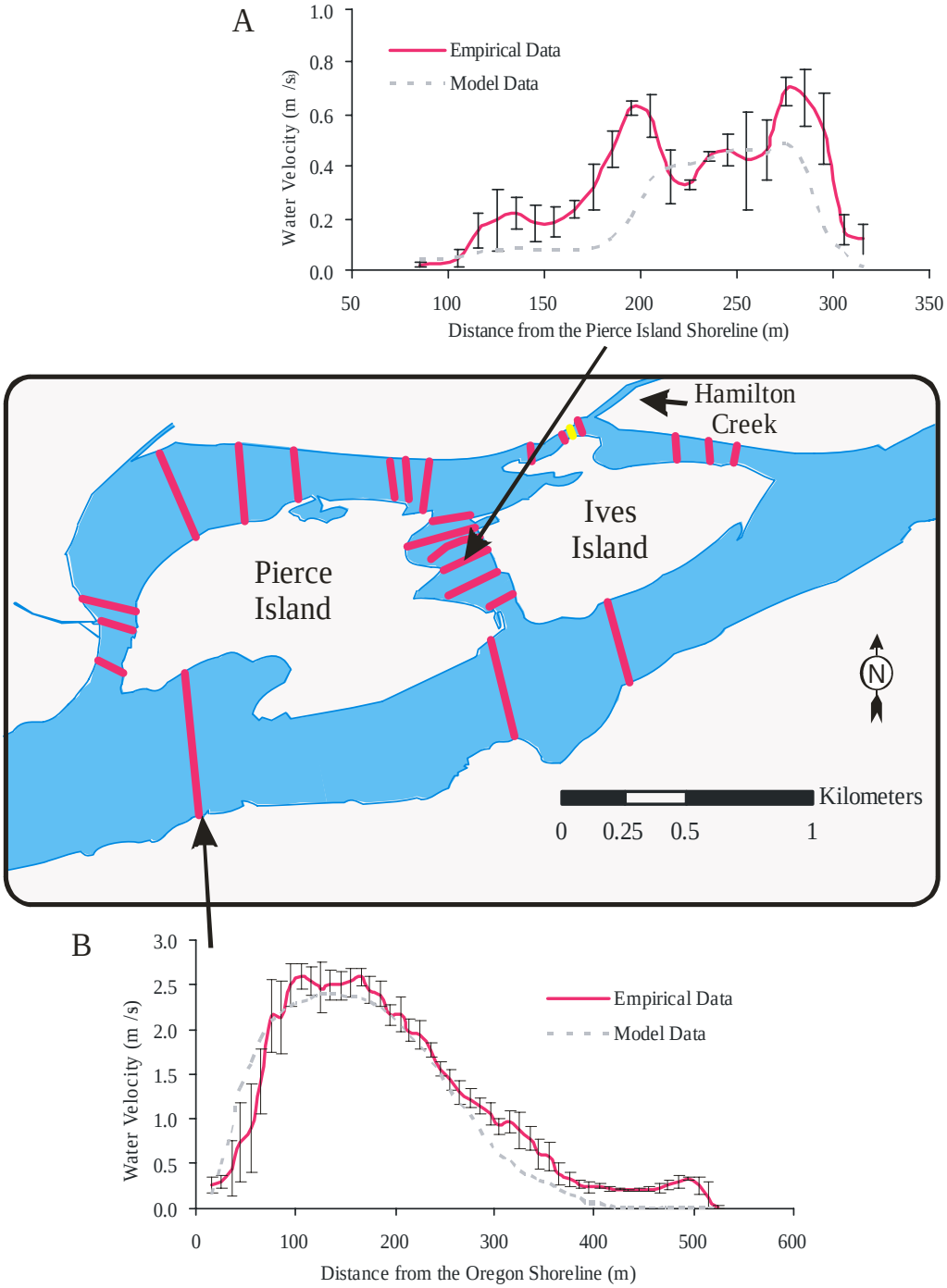

Figure 6. – Locations of the empirical water velocity transects. Graphs show profiles of the root mean squared values for empirical and model velocity data along the transects for a transect with poor agreement (A), and good agreement (B) between empirical and modeled data. Vertical bars are the standard deviations of the empirical data. The yellow transect highlights the one area where empirical and modeled data did not agree. All values are significant at $P < 0.05$.

observations had modeled WSEs less than those observed empirically and the rest were greater than those observed. The average for the absolute value of the differences between the modeled and empirically collected WSE data was 0.10 m (SD 0.07). The largest RMSE value was 0.16 for the collection date of 19 June 2000 (Figure 4).

Eighty-one beach seine sets were made (38 in sampling period 1 and 43 in period 2) to validate subyearling rearing area predictions. A total of 2,620 subyearlings were caught, 1,038 in period 1 and 1,582 in period 2. The percentages of beach seines that caught no subyearlings were 15.8% for period 1 and 18.6% for period 2. The average length of subyearlings was 43 mm (SD = 7) and 55 mm (SD = 13) for sampling period 1 and 2, respectively. Predictions of subyearling presence in rearing areas using logistic regression were validated with the beach seine data and resulted in an overall accuracy of 80% (Table 4). Subyearling presence in rearing areas was predicted with higher accuracy than their absence (Table 4).

Table 4. – Classification accuracy of subyearling presence and absence in predicted rearing areas as validated with catch data from beach seining. Producer's accuracy indicates how well empirical catch data classified with the simulated rearing areas. User's accuracy indicates the probability that locations from the rearing grids actually classified correctly with the empirical catch data.

	Beach Seine Data Classification		
Model Classification	Presence	Absence	Row Total
Presence	57	10	67
Absence	6	8	14
Column Total	63	18	81

Producer's Accuracy		User's Accuracy	
Presence	= 90%	Presence	= 85%
Absence	= 44%	Absence	= 57%

Overall Accuracy = (57 + 8)/81 = 80%

Our beach seining revealed spatial differences in catch locations between the two sampling periods. Skamania Island was the location of the highest subyearling catches during period 1. In period 2, most fish were caught in the upper half of the Bonneville study area around Ives and Pierce islands (Figure 7). Locations where fish were absent were relatively consistent between the two sampling periods. Our predictions of suitable subyearling rearing area for the entire Bonneville study area, as well as the individual reaches, were strongly and

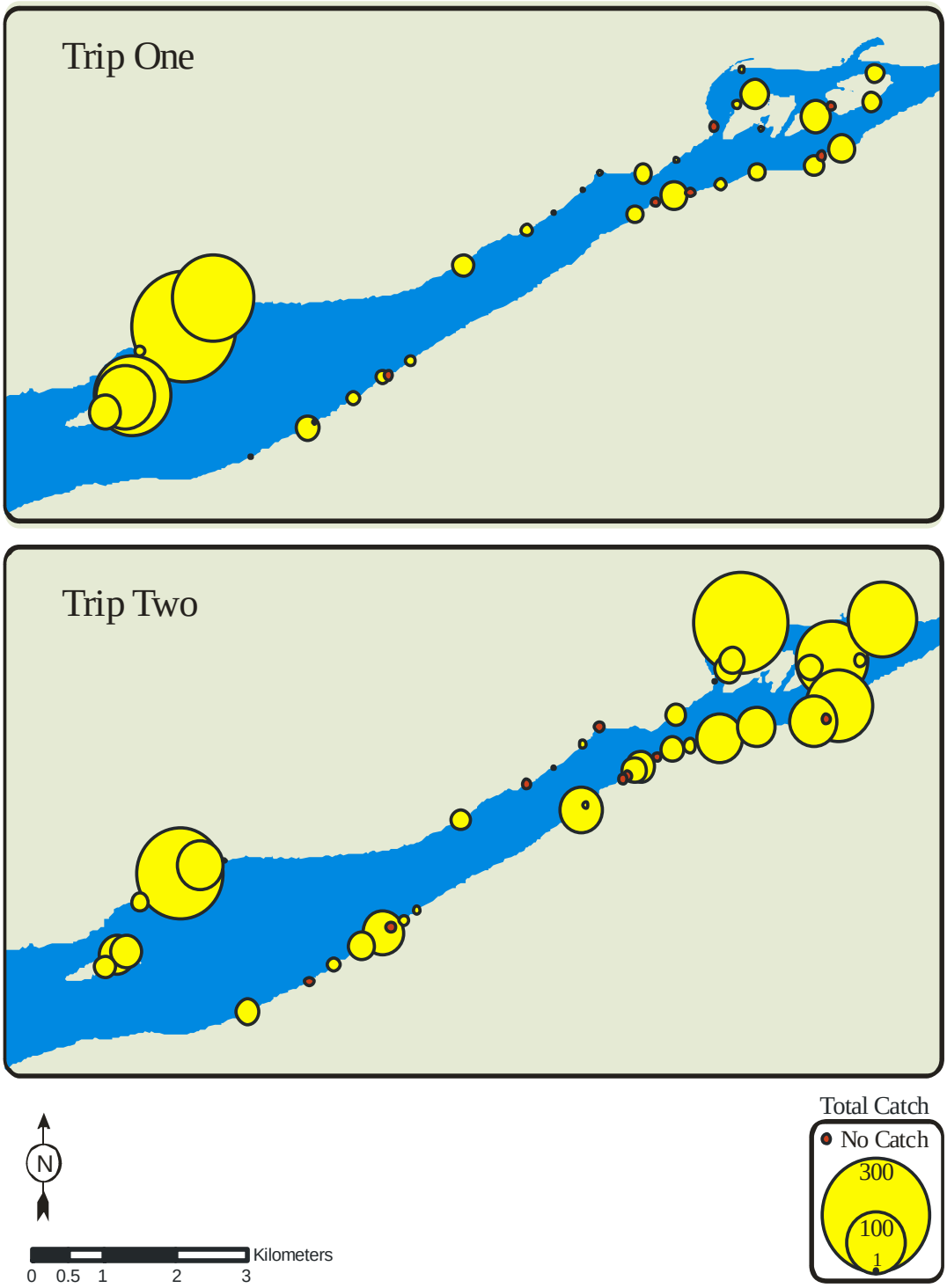

Figure 7. – Locations and numbers of subyearlings caught during beach seining trips one and two in 2003 in the Bonneville study area.

negatively related to both Bonneville Dam discharge and downriver WSE (Table 5). Graphically, the relationships between the hectares of subyearling rearing area and the independent variables were curvilinear and inversely related (Figure 8). The temporal trends in hourly predictions of hectares of rearing area indicated an overall decrease in subyearling rearing areas as the study period progressed and the overall discharge pattern increased (Figure 9).

Table 5. – Spearman's correlation coefficients r^2 for the relationships between hectares of subyearling rearing areas, Bonneville Dam discharge, and downriver WSE for the Bonneville study area and the upper, lower, islands, and main-channel reaches. All coefficients were significant with a $p < 0.05$.

Study Reaches	Discharge	WSE
Bonneville Study Area	0.97	0.97
Upper	0.95	0.95
Lower	0.95	0.98
Islands	0.98	0.95
Main-channel	0.95	0.98

Comparisons of hectares of subyearling rearing area between reaches show island areas contain less absolute rearing area than the main-channel, and that the upper reach contained more hectares than the lower reach (Table 6). However, when the hectares of subyearling rearing areas are standardized by the total length of shoreline, island areas contain more rearing hectares per kilometer than does the main shoreline (Table 6). Standardization had little effect on the number of rearing hectares in the upper and lower reaches (Table 6). The Mann-Whitney test showed significant differences in the hectares per kilometer of subyearling rearing areas between the island and the main-channel ($Z = -46.7$; $P < 0.000$), and between the upper and lower reaches ($Z = -22.0$; $P < 0.000$).

The spatial pattern of persistent subyearling rearing areas was not uniform within the Bonneville study area during 2003. The majority of the most highly persistent areas under the range of flows we examined were located on Pierce and Ives islands (Figure 10). Skamania Island, particularly the downriver end, also had a significant portion of persistent subyearling rearing area. Most of the shorelines on the main-channel contained less rearing area, especially at locations with steep or rip-rapped shorelines (e.g., the lower half of the Bonneville study area on the Oregon shoreline), and in areas with bedrock (e.g., the entire Oregon shoreline across from, and upstream of, Ives Island; Figure 10). One other location with sparse subyearling rearing area was located on the Washington main-channel shoreline approximately 1.5 km downstream of Pierce Island. This is an area with coarse substrates, steep slopes, and deep water near the shoreline.

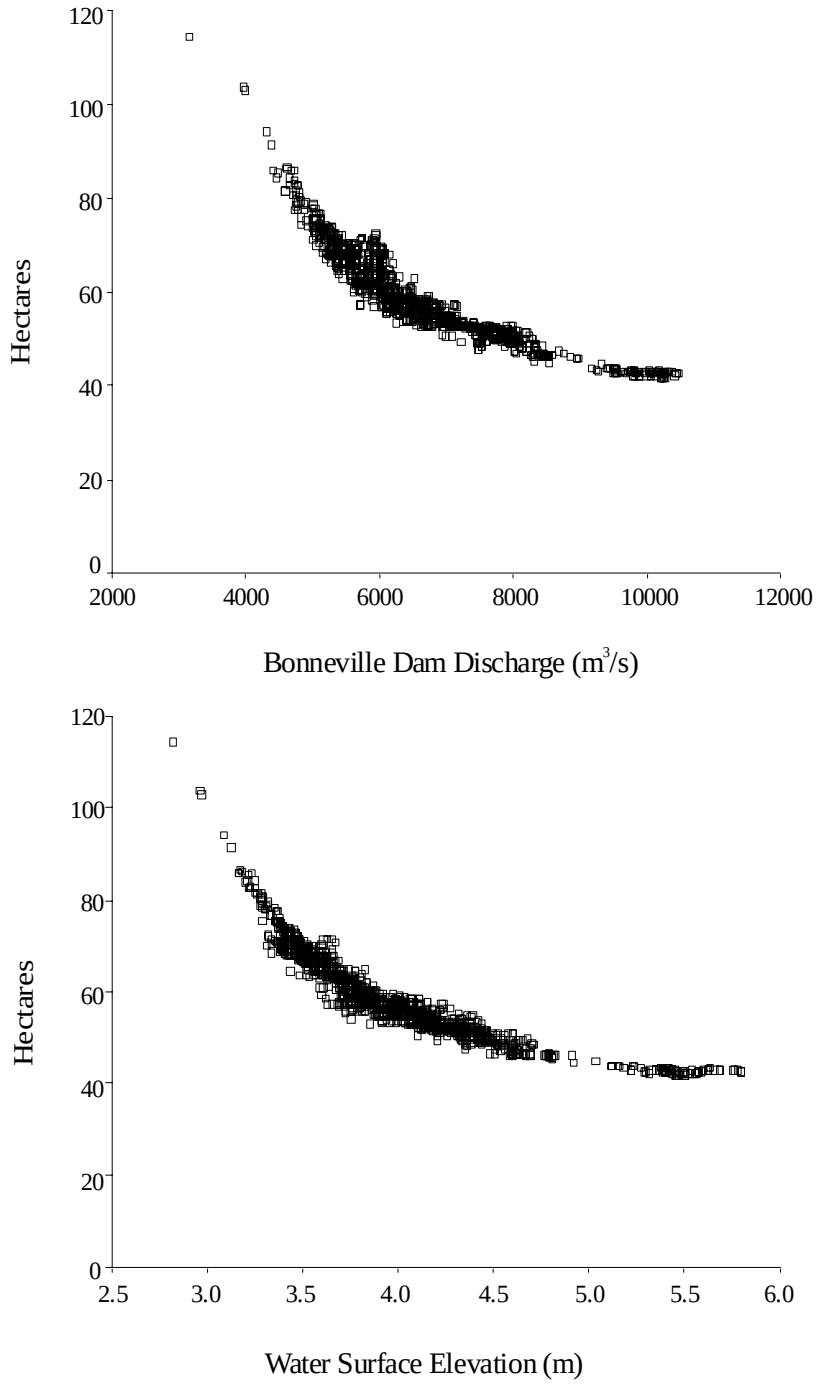

Figure 8. – Graphs showing the relationships between the hectares of subyearling rearing areas to Bonneville Dam discharges and downriver WSE for the Bonneville study area.

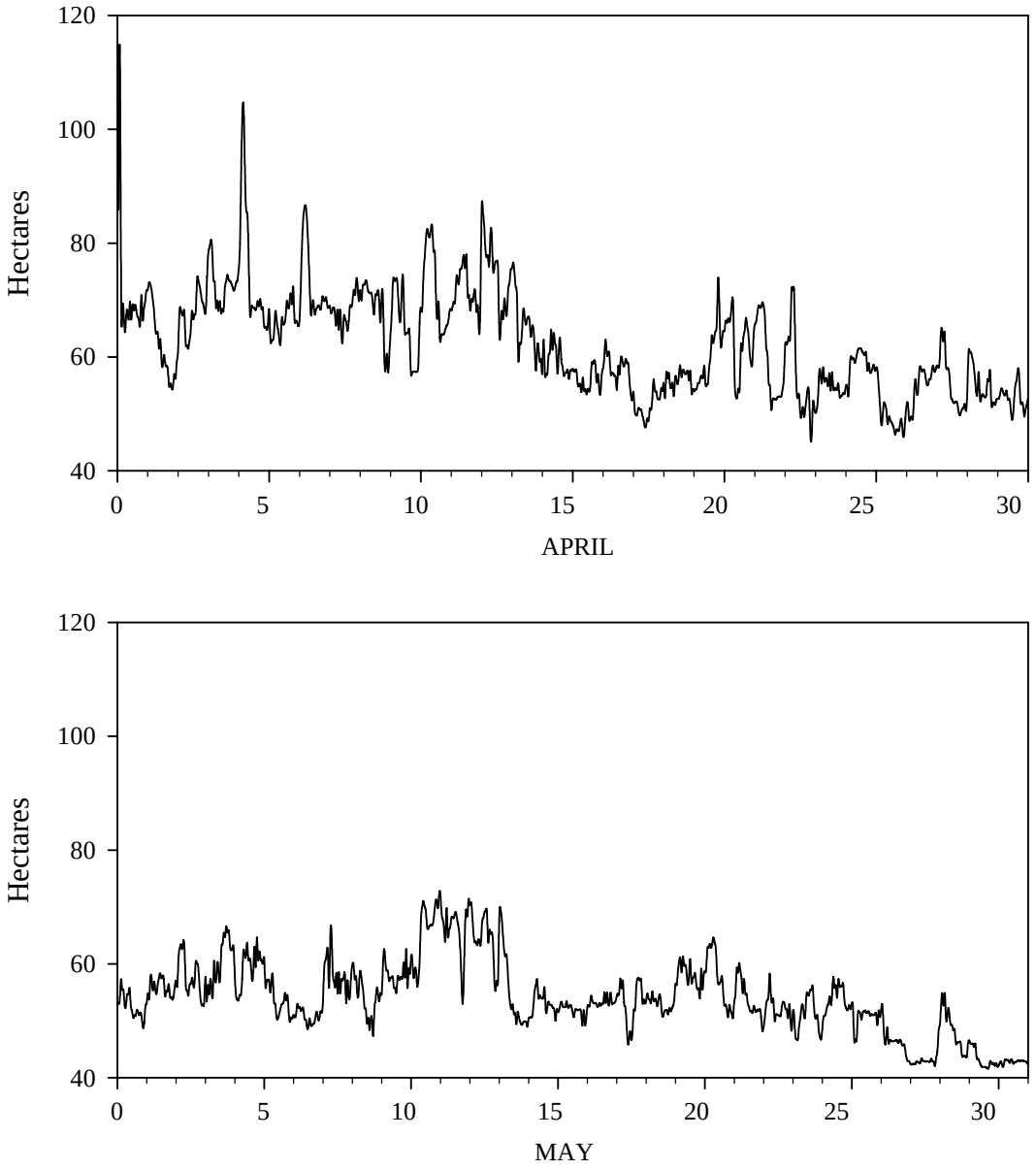

Figure 9. – Graph of the temporal trend in hourly hectares of subyearling rearing areas for the Bonneville study area in the months of April and May, 2003.

Table 6. – Percent difference between island and main-channel, and upper and lower reaches, for hectares and hectares standardized by the kilometers of shorelines of subyearling rearing areas.

	Percent Hectares		Percent Hectares/Kilometer	
	Island/Main-Channel	Upper/ Lower	Island/Main-Channel	Upper/ Lower
Mean	89	116	195	114
Standard Deviation	5	9	14	9
Minimum	71	89	121	69
Maximum	106	140	239	138

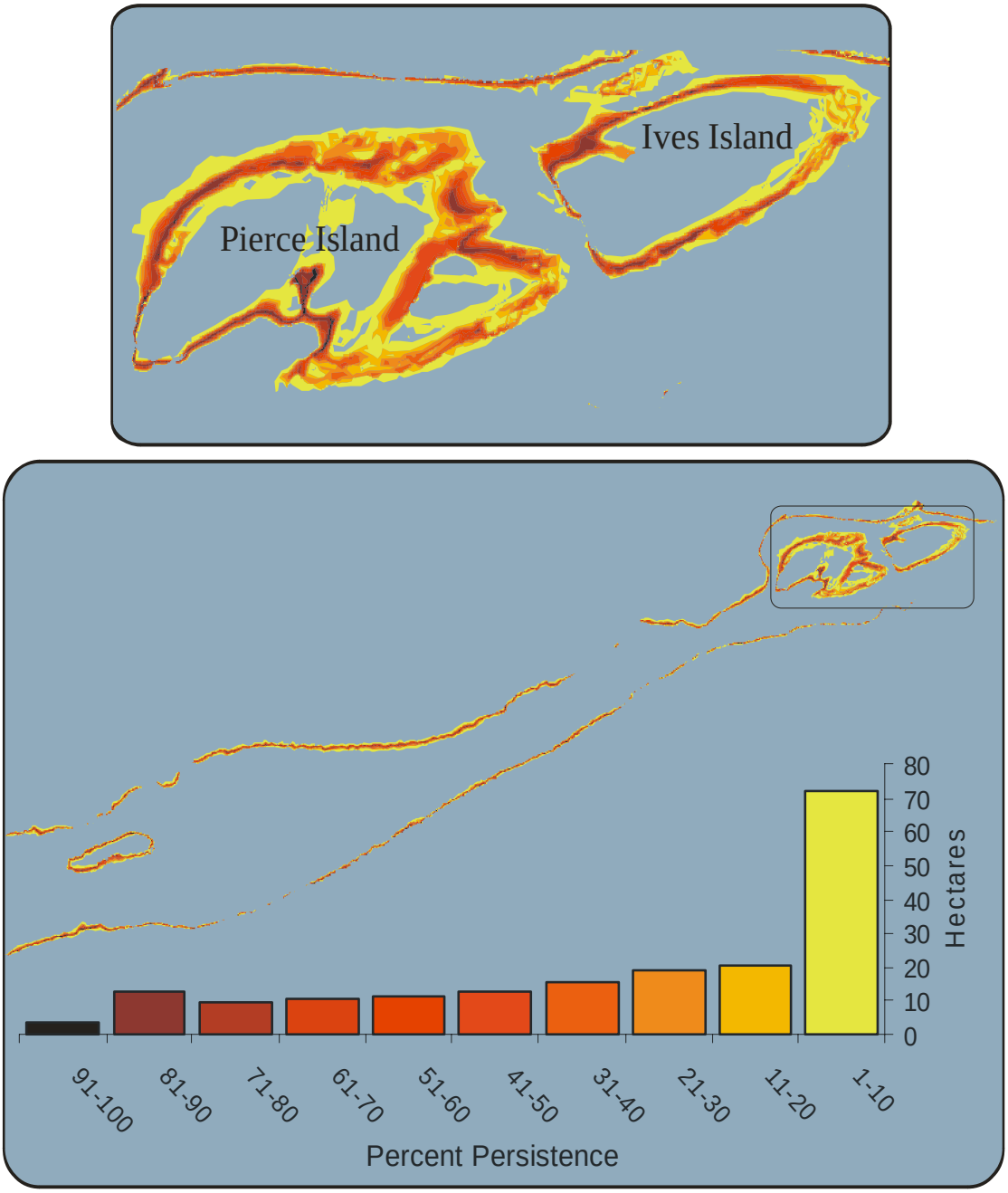

Figure 10. – Percent persistence map of subyearling rearing areas for the study period and total hectares of percent persistence groupings for the Bonneville study area. Darker areas indicate areas having higher persistence of subyearling rearing over the two month study period than lighter areas.

Approximately half of all hourly time intervals modeled during the two-month study period had corresponding decreases in either discharge or WSE. Of the 1,464 hourly simulations during the study period, 726 (50%) and 748 (51%) showed decreases in discharge or WSE, respectively. Of the hourly intervals that had decreases in discharge, 149 (10%) had an increase in WSE. Additionally, 583 had predicted dewatered areas greater than 0.5 hectares. Of the hours modeled with no decreases in discharge or had increases discharge, 216 had corresponding decreases in WSE.

Analysis of dewatering events showed significant relationships between the size of ΔQ and ΔW and the number of hectares dewatered. The amount of dewatered area was moderately correlated with both ΔQ and ΔW (Figure 11; Table 7) for the total study area and all reaches (Table 7). The strongest correlations between the amount of dewatered area and ΔQ were in the islands and upper half of the Bonneville study area. Bivariate linear regressions also showed significant but weak relationships between the hectares dewatered and the independent variables ΔQ and ΔW (Table 8). Most dewatered areas of significant size were created at no, or only small, changes in ΔQ (Figure 11).

The spatial distribution of areas frequently dewatered was similar to the most persistent subyearling rearing areas. The highest frequency of repeated dewatering events occurred around Ives and Pierce Islands (Figure 12). Pierce Island had the most expansive area subjected to dewatering in the entire study area. Along the main-channel of the Columbia River and around Skamania Island, lesser amounts of dewatering occurred, particularly along the upper section of the Oregon shoreline. Overall, 78% of all dewatered areas was also initially predicted to be suitable for subyearling rearing (Table 9). Overlap between dewatered and subyearling rearing areas for the individual reaches of the Bonneville study area was also high, with the main-channel having the highest percentage of overlap and the upper reach having the lowest percentage of overlap (Table 9).

Dewatering also caused the formation of pools within distinct discharge ranges, although there was no relationship to changes in ΔQ (Figure 13). The largest pools were formed at discharges less than 6,760 m^3/s and discharges greater than 9,750 m^3/s (Figure 13), between which only a minor amount of pools was formed. Our modeling showed that pools only formed on Pierce and Ives islands during the study period, with 76% of the total pool area occurring on Pierce Island. The maximum area of pools in any hour was 1.8 hectares on Pierce Island.

The results from two years of stranding and entrapment evaluations by the Pacific States Marine Fisheries Commission (PSMFC 2004) shows that subyearlings were stranded and entrapped, with some resultant mortality, in the Bonneville study area. In 2003 and 2004, stranding and entrapment occurred mostly on Ives and Pierce islands (PSMFC 2004; Figure 14). Especially large entrapment events were documented on 11 May and 12 May, 2003 that entrapped 855 and 530 subyearlings, respectively (Duston and Wilson 2004). This event occurred in a large pool that forms at flows between approximately 5,000 and 6,200 m^3/s in area C (Figure 14). Based on PSMFC observations, more subyearlings were entrapped than were stranded, but entrapment resulted in a low percentage of mortalities (less than 1%). Conversely, stranded subyearlings resulted in over 88% mortality in both 2003 and 2004. The

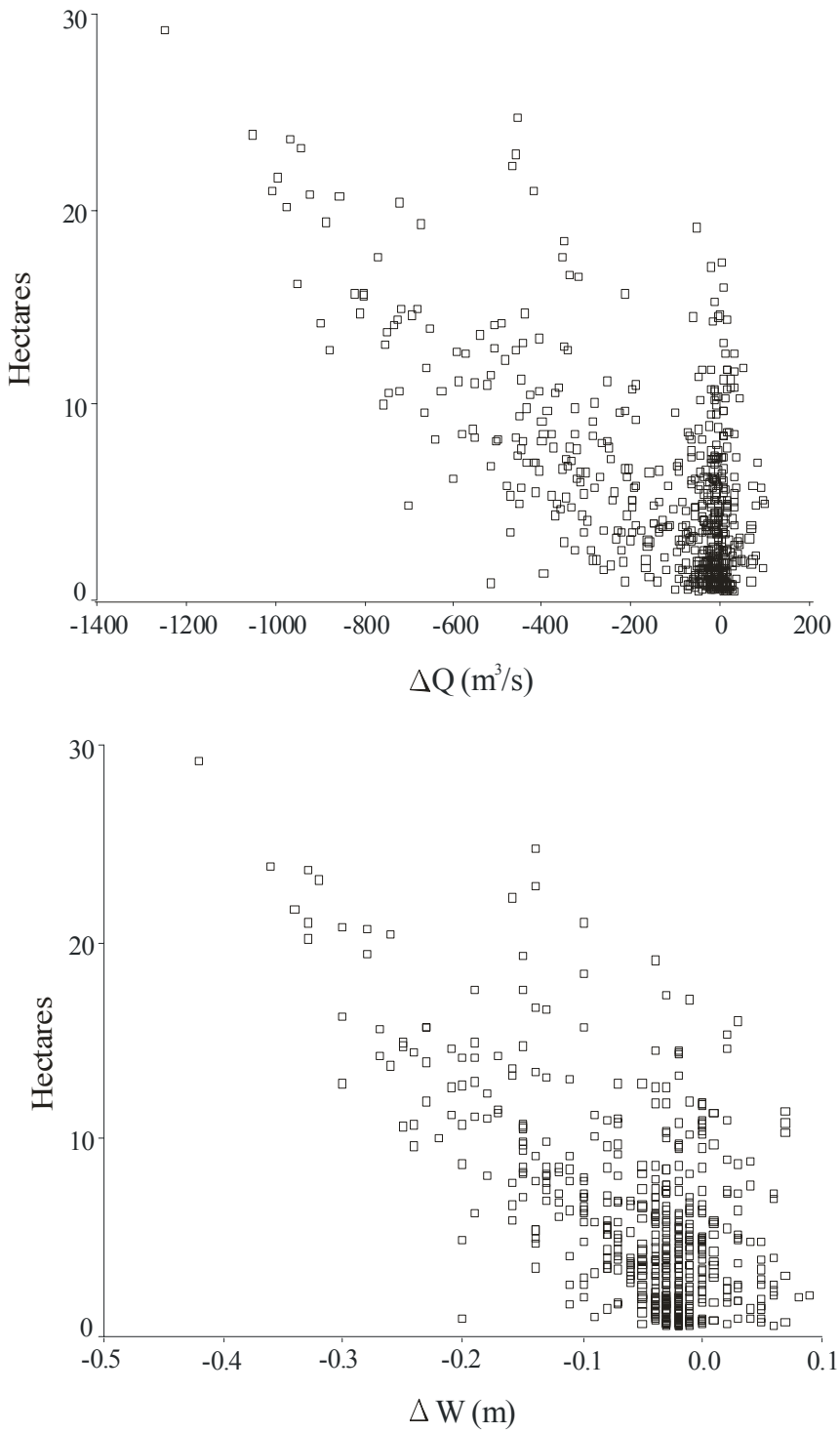

Figure 11. – Graphs of the relationships between the hectares of dewatered area to hourly change in ΔQ and ΔW for the Bonneville study area.

Table 7. – Pearson's correlation coefficients r^2 results for dewatered hectares ΔQ, and ΔW for the Bonneville study area as well as the upper, lower, island, and main-channel reaches. All coefficients were significant with a $P < 0.05$.

Study Reaches	ΔQ	ΔW
Bonneville Study Area	0.66	0.63
Upper	0.69	0.65
Lower	0.57	0.55
Islands	0.69	0.65
Main-Channel	0.59	0.57

Table 8. – Bivariate linear regressions r^2 results with the hectares of dewatered area as the dependent variable for the Bonneville study area and the upper, lower, island, and main-channel reaches. The independent variables used were ΔQ and ΔW. All bivariate linear regressions were significant with a $P < 0.05$.

Study Reaches	ΔQ	ΔW
Bonneville Study Area	0.43	0.38
Upper	0.47	0.43
Lower	0.32	0.30
Islands	0.47	0.42
Main-Channel	0.34	0.32

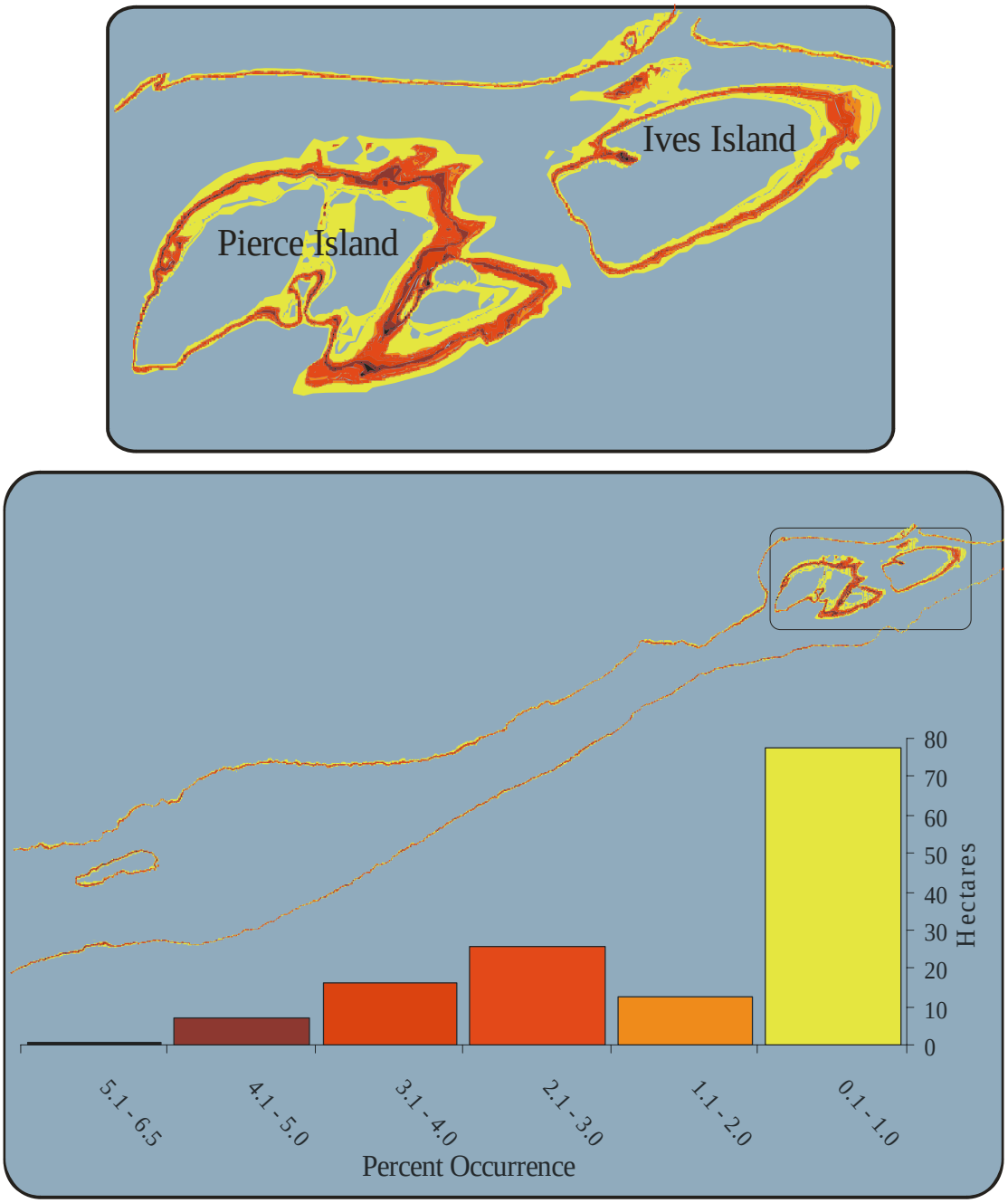

Figure 12. – Percent occurrence map of dewatered areas for the study period and total hectares of percent occurrence groupings for the Bonneville study area. Darker areas indicate areas having higher occurrence of dewatering events over the two month study period than lighter areas.

Table 9. – Minimum, maximum, mean, and standard deviations of the percentage of dewatered area that were initially good subyearling rearing areas for the Bonneville study area as well as the upper, lower, island, and main-channel reaches.

Study Reaches	Minimum Percentage	Maximum Percentage	Mean Percentage	Standard Deviation
Bonneville Study Area	42	100	78	11
Upper	42	100	73	14
Lower	58	100	87	3
Islands	42	100	75	14
Main-Channel	48	88	84	3

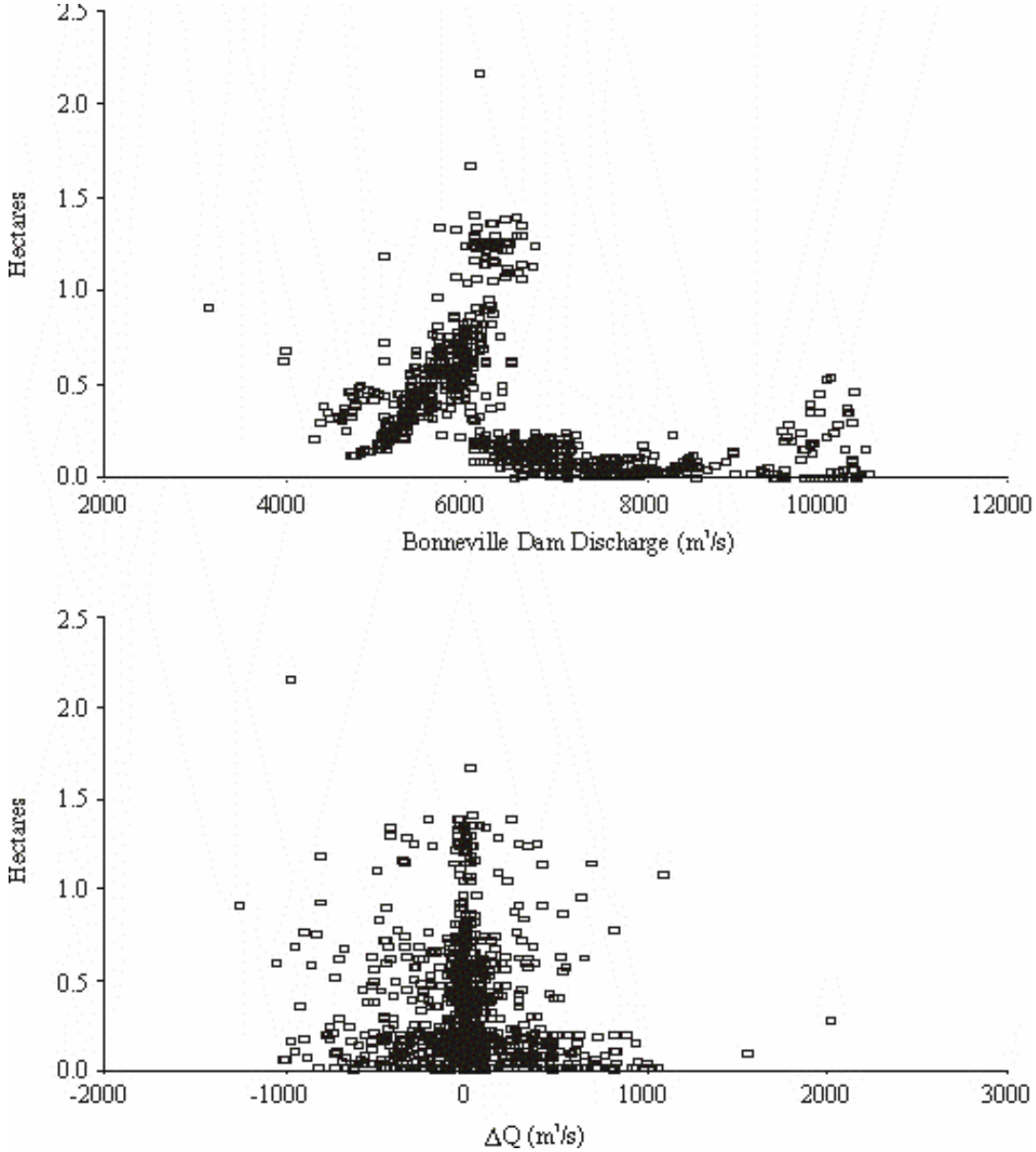

Figure 13. – Hectares of pools for the entire Bonneville study area related to Bonneville Dam discharge and hourly changes in discharge.

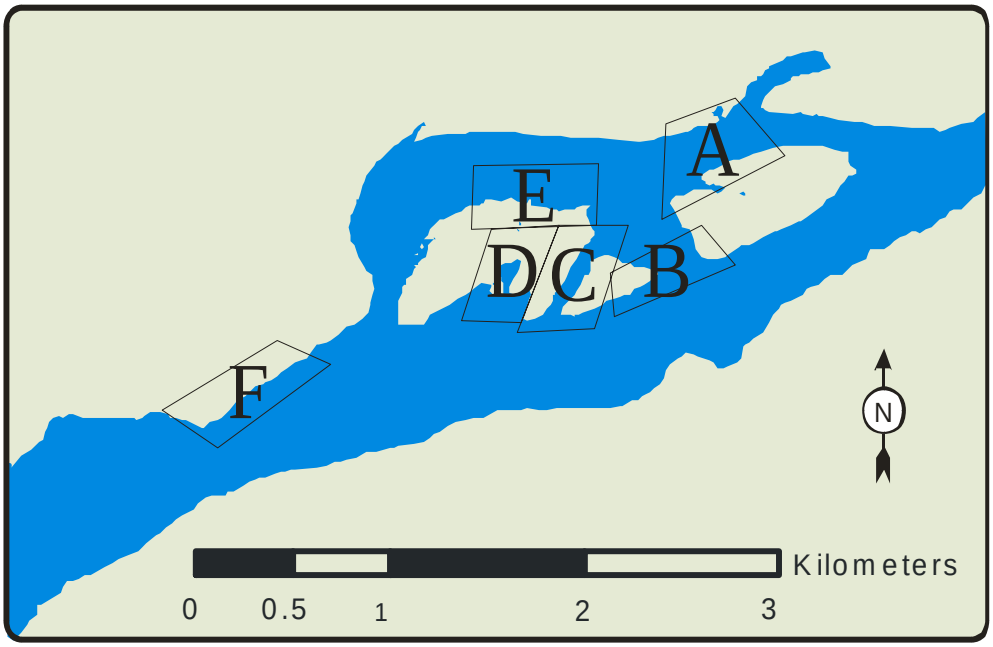

Sample Area	2003 Entrapment Catch		2003 Stranding Catch	
	Total	Mortalities	Total	Mortalities
A	71	25	8	5
B	249	0	0	0
C	114	5	4	4
D	25	0	2	2
E	253	7	0	0
F	1	0	0	0
Unknown	3,341	0	11	11

Sample Area	2004 Entrapment Catch		2004 Stranding Catch	
	Total	Mortalities	Total	Mortalities
A	1,244	1	110	95
B	19	0	2	2
C	851	0	3	3
D	2	0	0	0
E	1,652	27	287	287
F	32	0	0	0
Unknown	0	0	3	3

Figure 14. – Sample areas, total catch, and mortalities of subyearlings from entrapment and stranding in the Bonneville study area for 2003 and 2004 (PSMFC 2004).

locations of stranding and entrapment areas occurred in areas were frequently dewatered and that were also important rearing areas (Figure 12; Figure 14).

Discussion

There is a long history of integrating a water velocity model with fish habitat criteria to examine relationships between water management and fish habitat. In the past, most studies used a one-dimensional hydrodynamic model to simulate the physical environment and applied habitat suitability criteria for target species or species assemblages. For example, Rubin et al. (1991) developed habitat suitability curves for juvenile Chinook salmon and steelhead using measures of depth, substrate, and velocity. Freeman et al. (2001) used a one-dimensional water velocity model to simulate temporally variable habitat availability for juvenile fish assemblages in the Tallapoosa River in the southeastern United States. The most widely used approach in North America to combine one-dimensional water velocity information and biological suitability data are the set of computer data that comprise the physical habitat simulation model (PHABSIM; Rieser et al. 1989; Kondolf et al. 2000). However, one-dimensional water velocity models are often inappropriate to use in rivers with complex channel forms and flow patterns such as back-eddies.

More recently, two-dimensional hydrodynamic models provide the physical parameters needed for modeling fish habitat altered by anthropogenic changes in river discharges. Leclerc et al. (1995) modeled juvenile Atlantic salmon (Salmo salar) in the Moisie River Quebec to determine the minimum flow needed to preserve Atlantic salmon habitat. Bowen et al. (2003) used a two-dimensional model to investigate the potential effects of channel modification on shallow, low-velocity habitats of young salmonids in the Yellowstone River. Tiffan et al. (2002) modeled a range of flows in the Hanford Reach of the Columbia River to quantify discharge-related changes in subyearling rearing areas.

Leclerc et al. (1995) noted that one of the advantages of two-dimensional water velocity modeling is that the spatial resolution can be adapted to the scale of an individual fish. This would be advantageous in modeling the abundance of a fish species at precise locations. Modeling at the scale of the fish would require incorporation of such meso-scale topographic features as boulders, root-wads and other flow obstructions (Crowder and Diplas 2000). Crowder and Diplas (2000) noted that leaving out such functionally important structures could change abundance results. We did not incorporate meso-scale structures (e.g., boulders, root-wads, other flow obstructions) into our two-dimensional hydrodynamic models because of the large size of the study area and logistical limitations. However, this is likely of little consequence since we did not attempt to model the abundance of subyearlings, rather only the spatiotemporal patterns of potential presence or absence. Huston (2002) found that using a lower spatial resolution, which does not include meso-scale structures, is appropriate for modeling species presence and absence. Therefore, despite the shortcomings of this approach, we were able to identify important habitat areas and to quantify relative discharge-related habitat changes for the 1-h time increments.

Our results show high overall agreement between empirical fish location data and the areas predicted to be suitable for subyearlings indicating that the subyearling rearing model

we used was applicable to the Bonneville study area. In the Bonneville study area, the overall correct prediction rate was 80%. This compares to an overall correct prediction rate of subyearling presence and absence in the Hanford Reach of 76%. We also found there was a greater number of subyearlings present in areas predicted not to have fish (43%) than in the Hanford Reach (31%). This is likely due to the differences in gear type and efficiency used to sample fish in the two areas, namely the beach seining used in the Bonneville study area samples a larger area than the point electrofishing used in the Hanford Reach. In addition, the validation approach in the Bonneville study area used a GIS-based comparison rather than statistical cross-validation using the logistic regression model. Nevertheless, the accuracy of the results, particularly in predicting subyearling presence, indicates that the rearing results for the Bonneville study area are robust.

Decreases in either discharge or WSE increase the rearing area available to subyearlings in the Bonneville study area. This finding is similar to other research that has shown subyearling rearing areas increase with decreasing discharge (Glova and Field-Dodgson 1995; Tiffan et al. 2002). As discharge decreases, water velocities in the littoral zone decrease, increasing the suitability and amount of available shoreline habitat. Additionally, the islands in our study area were important in providing littoral habitat for rearing subyearlings. Islands and main-channel backwaters were locations with the highest beach seine catches of subyearlings and the largest areas of persistent rearing habitat (Figure 7; Figure 10). The relatively flat topography of the islands provided low-velocity, littoral habitats over a range of flows, which contributed to the predicted persistence of the rearing habitat found there.

Our analysis of hourly dewatering supports the hypothesis that the amount of area dewatered and the magnitude of change in hourly Bonneville Dam discharge are related. There were a large number of instances when substantial areas were dewatered when ΔQ was small (<100 m^3/s) or near zero (Figure 11). This possibly resulted from large decreases in the downstream WSE caused by tidal cycles, which complicated bivariate relationships between dewatering, discharge, and WSE. Although both change in discharge and WSE were significantly correlated to the number of hectares dewatered in our bivariate comparisons, WSE was less important to dewatering. Although WSE may modify the amount of area dewatered at small changes in discharge, decreases in discharge are likely the driving factor in the creation of dewatered areas. Island areas contained the greatest amount of area dewatered compared to main-channel shorelines. This is important because islands provided suitable and persistent subyearling rearing areas (Figure 10; Figure 12).

Rapid changes in discharge to generate hydroelectric power results in downstream fluctuations in the littoral zone that affect both aquatic insect and fish communities and habitat use (Cushman 1985; Ferrington 1993; Valentin et al. 1996; Dare and Hubert 2002). Furthermore, rapid water recession from shoreline habitats cause direct mortality of fish by stranding or entrapment in pools (Saltveit et al. 2001; Nugent et al. 2002), the underlying behavioral and discharge-related mechanisms remain poorly understood. Saltveit et al. (2001) related stranding mortality of wild subyearling and yearling Atlantic salmon and brown trout (*Salmo trutta*) to water temperature, season, and time of day, and recommended reducing flows in a slow, stepwise manner to limit stranding and mortality. In contrast, Bradford

(1997) found that the rate of flow reduction was not a factor in stranding or entrapment of subyearlings in an artificial stream. In the Hanford Reach, Nugent et al. (2002) found subyearlings less than 81 mm were stranded and entrapped on gently sloped gravel bars and in pothole depressions, and that vulnerability was highest at night. The highest concentrations of subyearlings occurred in island complexes, which were also locations with high stranding and entrapment potential. Most subyearling mortality in the Hanford Reach resulted from entrapment in pools (Wagner et al. 1999).

Data collected by the PSMFC in the Bonneville study area documented stranding, entrapment, and subyearling mortality in areas we predicted to have the highest subyearling rearing persistence and highest number of dewatering events. The highest frequency of entrapment and stranding events occurs in sample areas A, C, and E (Figure 14). Large pools form in these areas during dewatering events, particularly in areas C and E. In sample area C, dewatering events occurred on 11 and 12 May, 2003 that formed a large pool, which entrapped 1,449 and 600 juvenile salmon (mostly subyearlings), respectively. Coho and chum were also entrapped (Duston and Wilson 2004). This pool forms between Bonneville Dam discharges of 5,000 and 6,200 m^3/s. The large pool located in sample area E forms between Bonneville Dam discharges of 3,200 and 4,550 m^3/s. Entrapment generally affects more subyearlings than stranding, but stranding causes greater mortality. However, because the PSMFC sampling efforts were not comprehensive, the actual numbers of subyearling entrapped and associated mortality are likely greater than reported (Duston and Wilson 2002).

Our statistical and spatial results support our working hypotheses that subyearling rearing and dewatering areas are sensitive to changes in Bonneville Dam discharge. Modeling water velocities, subyearling rearing areas, and dewatered areas required simplification and reduction of a multitude of interrelated environmental variables, which limited the resolution and accuracy of our results. Additionally, the dynamic nature of both the temporal and spatial trends in subyearling rearing and dewatered areas highlighted the difficulties in identifying a small number of environmental variables upon which to make habitat predictions and establish trends. However, the strong agreement observed between empirical data and modeled results suggests the utility of the approaches used, the outcomes observed, and the implications for management of complex hydrosystems such as the Columbia River below Bonneville Dam.

Management Implications

Empirical data showed that stranding or entrapment events do occur in the areas where we found high persistence of subyearling rearing area and large occurrences of dewatering events. Both the literature and this study show that dewatered areas usually overlap with habitat areas for subyearlings, and that dewatering can result in mortalities. Quantitative rules on ramping rates of discharge, physical habitat criteria, and numbers of mortalities of subyearlings related to these metrics are needed to provide mortality risk estimates. We found that the highest potential for entrapment pool formation occurs at specific discharge thresholds in the Bonneville study area. Specifically, large decreases in discharge created more dewatered areas, especially around Pierce and Ives islands. Our results suggest hydroelectric and fishery managers should minimizing the rate and magnitude of flow

fluctuations, especially at flows greater or less than the pool thresholds observed in this study. Finally, limiting fluctuations during the night could reduce the risk to subyearlings during this portion of the diel cycle, which the literature suggests has the potential for greater risk of stranding and entrapment.

References

Basu, A., and S. Malhotra. 2002. Error detection of bathymetry data by visualization using GIS. Ices Journal of Marine Science 59:226-234.

Bovee, K. D., and M. L. Scott. 2002. Implications of flood pulse restoration for Populus regeneration on the Upper Missouri River. River Research and Applications 18:287-298.

Bottom, D.L., C.A. Simenstad, A.M. Baptista, D.A. Jay, J. Burke, K.K. Jones, E. Casillas, and M.H. Schiewe. 2001. Salmon at river's end: the role of the estuary in the decline and recovery of Columbia River Salmon. U.S. National Marine Fisheries Service. 271 p.

Bowen, Z. H., K. D. Bovee, and T. J. Waddle. 2003. Effects of flow regulation on shallow-water habitat dynamics and floodplain connectivity. Transactions of the American Fisheries Society 132:809-823.

Bradford, M. J. 1997. An experimental study of stranding of juvenile salmonids on gravel bars and in side channels during rapid flow decreases. Regulated Rivers: Research and Management 13:395-401.

Buffington, J. M., and D. R. Montgomery. 1999. A procedure for classifying textural facies in gravel-bed rivers. Water Resources Research 35:1903-1914.

Chapman, W. M. 1943. The spawning of chinook salmon in the main Columbia River. Copeia 3:168-170.

Crowder, D. W., and P. Diplas. 2000. Using two-dimensional hydrodynamic models at scales of ecological importance. Journal of Hydrology 230:172-191.

Cushman, R. M. 1985. Review of ecological effects of rapidly varying flows downstream from hydroelectric facilities. North American Journal of Fisheries Management 5:330-339.

Dare, M. R., and W. A. Hubert. 2002. Changes in habitat availability and habitat use and movements by two trout species in response to declining discharge in a regulated river during winter. North American Journal of Fisheries Management 22:917-928.

Dauble, D. D., T. P. Hanrahan, D. R. Geist, and M. J. Parsley. 2003. Impacts of the Columbia River hydroelectric system on main-stem habitats of fall Chinook salmon. North American Journal of Fisheries Management 23:641-659.

Dauble, D. D., T. L. Page, and J. R.W. Hanf. 1989. Spatial distribution of juvenile salmonids in the Hanford Reach, Columbia River. Fishery Bulletin 87:775-790.

DeMers, M. N. 2002. GIS modeling in raster. John Wiley and Sons, New York.

Duston, R. and J. Wilson. 2002. 2002 evaluation of chum, chinook, and coho salmon entrapment near Ives Island in the Columbia River, Annual Report to the Bonneville Power Administration, Contract 00004287, Portland.

Duston, R. and J. Wilson. 2004. Record numbers of entrapped salmon discovered, May 12 and 13. Available: http://www.fpc.org/spawning/recordstrandings.pdf (April 2004).

Everest, F. H., and D. W. Chapman. 1972. Habitat selection and spatial interaction by juvenile chinook salmon and steelhead in two Idaho streams. Journal of the Fisheries Research Board of Canada 29:91-100.

Ferrington, L. C. J. 1993. Endangered rivers: A case history of the Arkansas River in the central plains. Aquatic Conservation: Marine and Freshwater Ecosystems 3:305-316.

Freeman, M. C., Z. H. Bowen, K. D. Bovee, and E. R. Irwin. 2001. Flow and habitat effects on juvenile fish abundance in natural and altered flow regimes. Ecological Applications 11:179-190.

Garland, R. D., K. F. Tiffan, D. W. Rondorf, and L. O. Clark. 2002. Comparison of subyearling fall chinook salmon's use of riprap revetments and unaltered habitats in Lake Wallula of the Columbia River. North American Journal of Fisheries Management 22:1283-1289.

Garland, R. D., K. F. Tiffan, D. W. Rondorf, J. Skalicky, and D. R. Anglin. 2003. Assessment of chum and fall chinook salmon spawning habitat near Ives and Pierce Islands in the Columbia River. Annual Report to the Bonneville Power Administration, Contract 1999003, Portland.

Ghanem, A., P. Steffler, F. Hicks, and C. Katopodis. 1996. Two-dimensional hydraulic simulation of physical habitat conditions in flowing streams. Regulated Rivers: Research and Management 12:185-200.

Glova, G. J., and M. S. Field-Dodgson. 1995. Behavioral interaction between chinook salmon and brown trout juveniles in a simulated stream. Transactions of the American Fisheries Society 124:194-206.

Graf, W. H. 1998. Fluvial hydraulics: flow and transport processes in channels of simple geometry. John Wiley and Sons., West Sussex, England.

Huston, M. A. 2002. Critical issues for improving prediction. Pages 7-21 *in* J.M. Scott, P.J. Heglund, M.L. Morrison, J.B. Haufler, M.G. Raphael, W.A. Wall and F.B. Samson, editors. Predicting species occurrences: issues of accuracy and scale. Island Press, Washington DC.

Hymer, J. 1997. Results of studies on chinook spawning in the mainstem Columbia River below Bonneville Dam. Washington Department of Fish and Wildlife. Columbia River Progress Report 97-9, Battleground.

Kondolf, G. M. 1997. Application of the pebble count: notes on purpose, method, and variants. Water Resources Bulletin 33:79-87.

Kondolf, G. M., E. W. Larsen, and J. G. Williams. 2000. Measuring and modeling the hydraulic environment for assessing instream flows. North American Journal of Fisheries Management 20:1016-1028.

Leclerc, M., A. Boudreault, J. A. Bechara, and G. Corfa. 1995. Two-dimensional hydrodynamic modeling: a neglected tool in the instream flow incremental methodology. Transactions of the American Fisheries Society 124:645-662.

Lillesand, T. M., and R. W. Kiefer. 2000. Remote sensing and image interpretation. John Wiley and Sons, New York.

NMFS (National Marine Fisheries Service). 1999. Endangered and threatened species: Threatened status for three chinook salmon evolutionarily significant units (ESUs) in Washington and Oregon, and endangered status for one chinook salmon ESU in Washington. Federal Register 64:14307-14328.

NOAA (National Oceanic and Atmospheric Administration). 2004. Endangered Species Act status of West Coast salmon and steelhead. Available http://www.nwr.noaa.gov/ 1salmon/salmesa/pubs/2pgr.pdf (May 2004).

Nugent, J., T. Newsome, M. Nugent, W. Brock, P. Wagner, and P. Hoffarth. 2002. Evaluation of juvenile fall chinook salmon stranding on the Hanford Reach of the Columbia River. Annual Report to the Bonneville Power Administration, Contract 9701400, Portland.

Orth, D. K. 1983. Aquatic habitat measurements. Pages 61-84 *in* L. A. Nielson, and D. L. Johnson, editors. Fisheries Techniques. American Fisheries Society, Bethesda.

PSMFC (Pacific States Marine Fish Commission). 2004. Chum, and other salmon species data for spawning areas in the Columbia River Basic. Available: http://www.fpc.org/ spawning_surveys.htm (June 2004).

Rieser, D. W., T. A. Wesche, and C. Estes. 1989. Status of instream flow legislation and practices in North America. Fisheries 14:22-29.

Rubin, S. P., T. C. Bjornn, and B. Dennis. 1991. Habitat suitability curves for juvenile chinook salmon and steelhead development using a habitat-oriented sampling approach. Rivers 2:12-29.

Saltveit, S. J., J. H. Halleraker, J. V. Arnekleiv, and A. Harby. 2001. Field experiments on stranding in juvenile Atlantic salmon (Salmo salar) and brown trout (Salmo trutta) during rapid flow decreases caused by hydropeaking. Regulated Rivers: Research and Management 17:609-622.

Steffler, P., and J. Blackburn. 2002. Two-dimensional depth averaged model of river hydrodynamics and fish habitat. University of Alberta, Edmonton.

Tiffan, K. F., R. D. Garland, and D. W. Rondorf. 2002. Quantifying flow-dependent changes in subyearling fall chinook salmon rearing habitat using two-dimensional spatially explicit modeling. North American Journal of Fisheries Management 22:713-726.

Valentin, S., F. Lauters, C. Sabaton, P. Breil, and Y. Souchon. 1996. Modeling temporal variations of physical habitat for brown trout (Salmo trutta) in hydropeaking conditions. Regulated Rivers: Research and Management 12:317-330.

van der Naald, W., R. Clark, and B. Spellman. 2002. Evaluation of fall chinook and chum salmon spawning below Bonneville, The Dalles, John Day, and McNary Dams. Annual report to the Bonneville Power Administration, Contract 1999-00301, Portland.

van der Naald, W., R. Clark, and B. Spellman. 2003. Evaluation of fall chinook and chum salmon spawning below Bonneville, The Dalles, John Day, and McNary Dams. Annual Report to the Bonneville Power Administration, Contract 1999-00301, Portland.

Venditti, D. A., M. A. Tennier, and D. W. Rondorf. 1996. Nearshore movements and feeding behaviors of juvenile fall chinook salmon in the Columbia River. Pages 80-97 *in* D. W. Rondorf, and K. F. Tiffan, editors. Identification of the spawning, rearing, and migratory requirements of fall chinook salmon in the Columbia River Basin, 1994. Annual Report to the Bonneville Power Administration, Contract DE-AI79-91BP21708, Portland.

Venditti, D. A., M. A. Tennier, and D. W. Rondorf. 1997. Nearshore movements of juvenile fall chinook salmon in the Columbia River. Pages 69-84 *in* D. W. Rondorf, and K. F. Tiffan, editors. Identification of the spawning, rearing, and migratory requirements of fall chinook salmon in the Columbia River Basin, 1995. Annual Report to the Bonneville Power Administration, Contract DE-AI79-91BP21708, Portland.

Wagner, P. G., J. Nugent, W. Price, R. Tudor, and P. Hoffarth. 1999. 1997-99 evaluation of juvenile fall chinook stranding on the Hanford Reach. Annual report to the Bonneville Power Administration, Contract 97BI30417, Portland.

Willmott, C. J. 1981. On the validation of models. Physical Geography 2:184-194.

Wolman, M. G. 1954. A method of sampling coarse river-bed material. Transactions of the American Geophysical Union 35:951-956.

CHAPTER TWO

Diel Spawning Behavior of Chum Salmon in the Columbia River

by

Kenneth F. Tiffan and Dennis W. Rondorf
U.S. Geological Survey
Western Fisheries Research Center
Columbia River Research Laboratory
5501A Cook-Underwood Road
Cook, Washington 98605, USA

and

Joseph J. Skalicky
U.S. Fish and Wildlife Service
Columbia River Fisheries Program Office
1211 SE Cardinal Court, Suite 100
Vancouver, Washington 98683, USA

Introduction

The Columbia River below Bonneville Dam supports a spawning population of chum salmon *Oncorhynchus keta* near Ives and Pierce islands, Washington (Hymer 1997). Although chum salmon are generally tributary spawners (Johnson et al. 1997), spawning has been documented in main-stem habitats of the Columbia River below the mouth of Hamilton Creek and elsewhere in the Ives Island area (van der Naald et al. 2003). With the listing of lower Columbia River chum salmon as "threatened" under the Endangered Species Act in 1999 (National Marine Fisheries Service 1999), much attention has been focused on monitoring and protecting this stock.

Chum salmon spawn in the Ives Island area in the fall when flows are at a seasonal low. Two nearby tributaries, Hamilton and Hardy creeks, whose flows are heavily dependent on precipitation, are often dry or contain too little water for fish to ascend to historical spawning grounds. Consequently, early-spawning fish are often restricted to a side channel of the Columbia River immediately downstream from the mouth of Hamilton Creek, where a significant amount of chum salmon spawning has occurred in the last 5 years (Garland et al. 2003; van der Naald et al. 2003). However, when Hamilton Creek is dry, flow through this channel is only maintained by discharges from Bonneville Dam that exceed 3,400 m^3/s (Garland et al. 2003).

Each year fishery managers must decide how much water to provide to sustain both chum salmon spawning and subsequent egg incubation while considering uncertain precipitation forecasts and other flow-related fishery management objectives. Since 1998, only minimal daytime flows have been provided to restrict spawning to lower riverbed elevations, which reduces the risk of dewatering spawning redds in the event of a subsequent decline in water availability. We use the term redd to refer to the collection of spawning nests made by an individual chum salmon. Even small reductions in discharge from Bonneville Dam have resulted in dewatering of chum salmon spawning redds in low-gradient spawning areas (Washington Department of Fish and Wildlife, unpublished data). Consequently, maintaining stable tail-water elevations at Bonneville Dam has become the goal of managing water for chum salmon spawning in the Ives Island area (Fish Passage Center 2003). However, this action provides little flexibility for passing more than the minimum spawning flows or for generating additional hydroelectric power. Furthermore, during years of high chum salmon abundance, low daytime flows reduce the area for spawning and may reduce population productivity through redd superimposition.

At present, a balance of fisheries and regional power needs is achieved by maintaining low, stable flows during the day and passing more water at night when the need arises. This water management strategy, referred to as reverse load following, is a conservative means of accommodating salmon spawning while minimizing the amount of water committed during subsequent egg incubation. It is currently used at Priest Rapids Dam to restrict fall Chinook salmon *Oncorhynchus tshawytscha* spawning to specific riverbed elevations during daytime in the Hanford Reach of the Columbia River (Federal Energy Regulatory Commission 1988). This practice has also been implemented at Bonneville Dam to pass more than the minimum spawning flows at night (U.S. Army Corps of Engineers 2003). Reverse load following is based on the

assumption that fish do not spawn at night, which is poorly established in scientific fact. However, if chum salmon do spawn at night, then spawning nests constructed at higher riverbed elevations under high nighttime flows could be dewatered at lower daytime flows. In addition, high nighttime flows may alter fish spawning behavior and habitat suitability if water velocities become too great. This study was initiated to assist in answering some of these fishery and flow management questions. Our objectives were to determine if chum salmon spawn at night in Columbia River habitats, and if there were diel differences in spawning behavior.

Study Area

We conducted our study below the mouth of Hamilton Creek, Washington in a side channel of the Columbia River, located between the Washington shore and Ives Island on the Columbia River at river kilometer 229 (as measured from the river's mouth; Figure 1). This channel is about 250 m long, has a mean width of 44 m, and longitudinal gradient of < 1%. The bed is composed of gravel (4-75 mm) and cobble (76-150 mm) substrate, and water velocities are generally < 1 m/s.

Methods

We used a dual-frequency identification sonar (DIDSON) to observe the diel spawning behavior of chum salmon from November 13 to December 6, 2003. The DIDSON was originally developed at the University of Washington's Applied Physics Laboratory for military use in harbor surveillance (Belcher et al. 2001), and has recently been used in fishery applications (Moursund et al. 2003; Tiffan et al. In press). It forms near-video-quality images by simultaneously transmitting and receiving acoustic beams. Because DIDSON images are created using sound instead of light, images can be produced in complete darkness or in turbid conditions. At a frequency of 1.8 MHz, images, or frames, are constructed from 96 beams, spaced 0.3° apart from each other in the horizontal plane. At this frequency, images can be formed to a range of 12 m, and resolution ranges from 3 mm at a distance of 1.5 m to 24 mm at a distance of 12 m from the camera. The field of view is 29° in the horizontal plane and 8.5° in the vertical plane. Images can be formed at a rate up to 12 frames/s. The DIDSON is 30 cm long, 20.5 cm high, and 17.5 cm wide, and weighs 5.5 kg in air but is slightly buoyant in water. Data collected by the DIDSON are sent via a cable to routing hardware where images can be output to video equipment or to a laptop computer using an Ethernet connection.

DIDSON displays of images enabled us to quantify various aspects of chum salmon behavior that would not have been possible with an ordinary underwater camera. Images are constructed by incorporating the distance of each object from the DIDSON based on the time differential between when acoustic signals are transmitted and received. The resulting view appears as if fish are observed from above, even though the DIDSON is oriented laterally toward their sides. Therefore, the field of view appears somewhat like a triangular-shaped plane in which fish positions, movements, and behaviors can be spatially quantified. In addition, alteration to the substrate (e.g., sediment plumes and cobble movement) can be detected. Distances and object sizes can be measured with the DIDSON software's measuring tool.

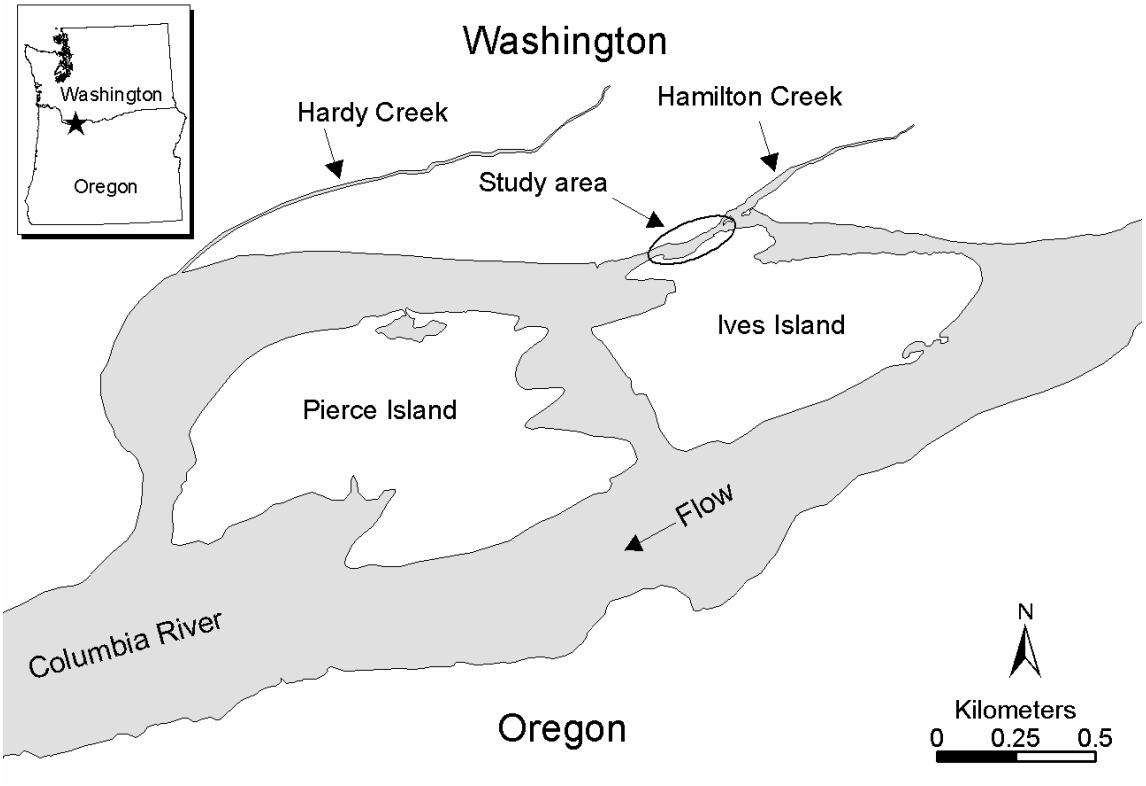

Figure 1.- Map of the area below the mouth of Hamilton Creek where the diel spawning behavior of chum salmon was observed in 2003. Fish also spawn in Hardy and Hamilton creeks when stream flows are adequate, and to a lesser extent around Ives and Pierce islands.

We mounted a DIDSON on a weighted bracket that allowed both horizontal and vertical adjustment of the DIDSON. The DIDSON was deployed on the riverbed in about 1 m of water and oriented perpendicular to the current. We usually set the length of the field of view to 4 m, which started 3 m in front of the DIDSON and extended to a maximum distance of 7 m. This field of view allowed us to clearly observe fish over the entire area of their spawning redd while maintaining a separation distance so as not to interfere with spawning behaviors. DIDSON images of spawning chum salmon were collected at a frequency of 1.8 MHz, which produced the highest resolution images, and were saved to laptop computer files at a rate of 8 frames/s. This frame rate produced clear, fluid images of fish movement and behavior while keeping file sizes manageable.

Pairs of chum salmon engaged in spawning behavior were opportunistically selected for observation. Because our study area was small and fish were abundant (>100 fish at any one time; Washington Department of Fish and Wildlife, unpublished data), finding spawning pairs for observation was relatively easy. Observers recorded the general locations of spawning fish during the day to facilitate locating fish during the day and night. We selected a pair of fish for observation if the female fish was actively digging a nest and a courting male was present, which suggested that the spawning act had likely not occurred. We positioned the DIDSON at a distance of about 5 m from the nest to avoid disturbing their behavior. This positioning also ensured the horizontal field of view was wide enough (about 2.5 m) to document the spatial extent of nest construction.

We collected data on various aspects of chum salmon spawning behavior in real-time to minimize the effort of subsequent image review and to confirm actual spawning events. These behaviors included 1) digging by the female fish, 2) tail crossing performed by the courting male fish, and 3) chasing intruding fish. We recorded the time of each female digging event to the nearest minute and marked its location on an acetate transparency attached to the laptop computer screen. The DIDSON software allowed us to display a grid of known scale over the field of view that we then transferred to the transparency to provide a reference for dig locations. We replaced transparencies hourly. We also recorded the number of times the courting male crossed over the peduncle of the female in 15-min increments. This tail-crossing behavior is a precursor to the spawning event (Tautz and Groot 1975; Helle 1981; Schroder 1981). The number of times that either the female or male fish chased other intruding fish was also recorded.

Because acoustic images did not allow us to see the release of gametes during a spawning act, we used four criteria to determine that a spawning event had occurred. First, the female and male fish would move along side each other and remain relatively motionless for 5-10 s. Second, there would be a complete cessation of tail crossing by the courting male after a spawning event. Third, there would be a rapid increase in the frequency of digs made by the female to cover newly deposited eggs. Fourth, the spatial pattern of covering digs made by the female fish would generally be shaped in an arc or cluster and would be located immediately upstream of the spawning location. These criteria were derived from observations of spawning chum salmon made by Tautz and Groot (1975) and Schroder (1981). Computer files of all suspected spawning events were subsequently reviewed for accuracy by two different observers. Deployment of an underwater video camera during daylight hours allowed us to verify each type of spawning behavior observed with the DIDSON.

Because we had no way of knowing how far along a pair of fish was in their spawning cycle, we observed each pair continuously until they spawned and thereafter for a minimum of an additional 1-2 h. For pairs that did not spawn according to our criteria, we ended observations when the male fish stopped active courtship or if digging by the female declined and became sporadic. After each observation period, we marked the redd location with a differentially-corrected global positioning system (GPS) and selected a new pair of fish for observation regardless of the time of day. We selected new spawning pairs that varied in space (GPS location) and time (30-40 h to complete a female's spawning cycle) to ensure that each pair had not been previously observed (Tautz and Groot 1975). In other words, areas where spawning fish were observed were not revisited for a period of 30-40 h.

Data were analyzed to test null hypotheses that spawning chum salmon exhibited no diel differences in digging, tail crossing, and chasing frequency. We defined daytime as the period from 0.5 h after sunrise to 0.5 h before sunset, and we defined nighttime as the period 0.5 h after sunset to 0.5 h before sunrise. We did not analyze data collected during the crepuscular periods (the 1-h periods encompassing sunrise and sunset), and only spawning pairs for which there was both day and night observations were included in analyses. Additionally, only pre-spawning behavioral data were included in analyses because the marked changes in digging and tail crossing following a spawning event are well established. Fish were categorized by their time of spawning as either day spawners, night spawners, or fish that did not spawn. We then examined the diel behavioral differences for each category of spawning fish. Data were first $\log_e$ transformed to better approximate normality. We then used two-way analysis of variance for unbalanced designs with time of spawning (i.e., day, night, none) and diel period (i.e., day or night) as the main effects. We tested the significance of the main effects as well as their interaction. We used Fisher's test for least significant differences to determine the significance of diel pair-wise comparisons within each spawning category (SAS Institute 2000). If no significant differences were found, we pooled the data from the spawning categories and compared mean diel spawning metrics using two-sample *t* tests. Statistical significance was assumed at $P < 0.05$.

The locations of individual digging events were recorded to determine the spatial extent of chum salmon spawning nests, and to test for diel differences in nest size. The locations of all digs made to construct a nest were digitized and incorporated in a geographic information system. We estimated the size of each nest by drawing the smallest possible polygon that encompassed the cluster of dig locations and calculating the area. Finally, we compared mean nest size between day and night using a two-sample t-test, and also calculated a grand mean area for all nests.

Results

We observed 14 different pairs of chum salmon continuously for 4.5 to 33 h. We collected 79 h of daytime and 111 h of nighttime observation excluding crepuscular periods. We documented spawning events for 10 different pairs of chum salmon, of which three pairs spawned twice. Of the 13 observed spawning events, nine occurred during the night and four

occurred during the day. Sufficient day and nighttime data existed for 11 pairs of fish to permit statistical analyses.

The DIDSON enabled us to observe each time a female chum salmon dug during nest construction. The digging event could be seen when the female fish would move slightly upstream and produce a plume of sediment that appeared as light cloud behind the fish (Figure 2). The cloud would then dissipate as the sediment moved downstream. Female chum salmon would generally dig over a broad area to construct nests that averaged 2.1 m^2 (range 1.1 to 2.9 m^2; Figure 3); there were no diel differences in nest size (t=-0.3974, P=0.7014). Toward the end of nest construction, digs were often concentrated in the area where eggs were subsequently deposited (Figure 3). Post-spawning digs made to cover the eggs were located immediately upstream of the spawning site, and were generally in a cluster or an arc-shaped pattern (Figure 3). Female chum salmon that constructed a second nest located it directly in front, or off to the side and upstream, of the first nest about 0.5 m away. We observed that the digs made to cover the first nest also served to partially excavate the second nest.

During the pre-spawning period of nest construction, the female would engage in continuous but variable digging activity (Figure 4). The mean number of pre-spawning digs per 15-min interval was 7.7 during the day and 7.5 during the night (Table 1). Immediately after spawning, the number of digs per 15-min interval rapidly increased to a mean peak of 64 (range 23 to 84, SD = 20.6, all data combined) and then returned to pre-spawning levels (Figure 4). Post-spawning covering digs were distinct from pre-spawning digs in that they were rapid, relatively small, and the female would quickly return to the point of egg deposition after each dig. We found no significant differences between behavioral metrics and daytime and nighttime pair-wise comparisons (F = 1.70; P = 0.2281). Similarly, a two-sample t test comparing mean day and night pre-spawning digging for all fish was not significant (t = 0.19; P = 0.8537; Table 1).

During spawning nest construction and courtship, the female and male fish were continuously moving and were never directly along side each other. The courting male generally held position behind the female and would cross her peduncle numerous times before approaching her to "quiver". The quiver was a lateral display in which the male fish would exhibit a series of high-frequency body flexures that gave it the appearance that it was vibrating (Schroder 1981). We observed quivering on our underwater video camera, but it was not distinguishable with the DIDSON. We observed tail crossing in all courting males, but it was highly variable over time (Table 1). Tail crossing ceased immediately after every spawning event, but would resume after the female completed her covering digs and began constructing her next nest (Figure 4). In one instance, tail crossing resumed within 15 minutes of the spawning event. We found no statistically significant diel differences in male chum salmon tail crossing behavior (ANOVA: F = 1.82, P = 0.2002; t-test: t = 0.33, P = 0.7413).

We could readily identify a chum salmon spawning event with the DIDSON because the courting male would swim quickly along side the female and both fish would remain motionless for 5-10 s. Often one or more satellite male chum salmon would rush in to spawn when the female and courting male began spawning. In one instance, we observed six males trying to

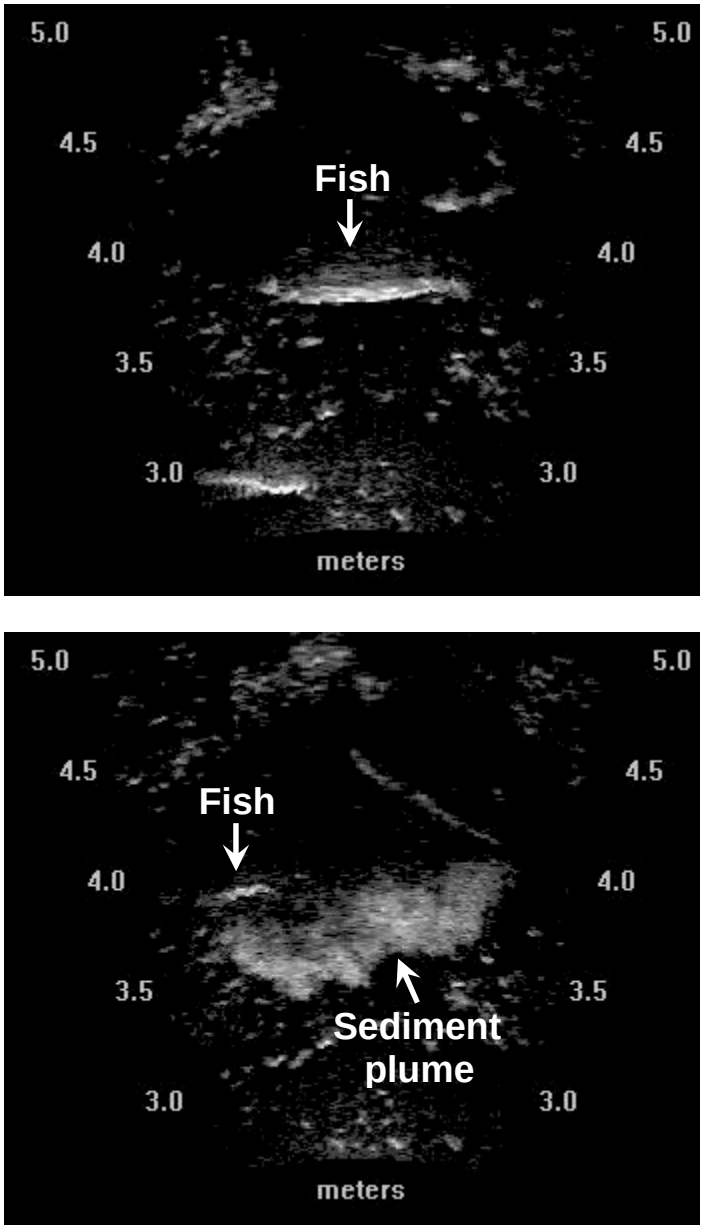

Figure 2.-An example of an acoustic image produced by the DIDSON of a digging event by a female chum salmon. The top panel shows the female fish before digging and the bottom panel shows the plume of sediment produced by the digging event.

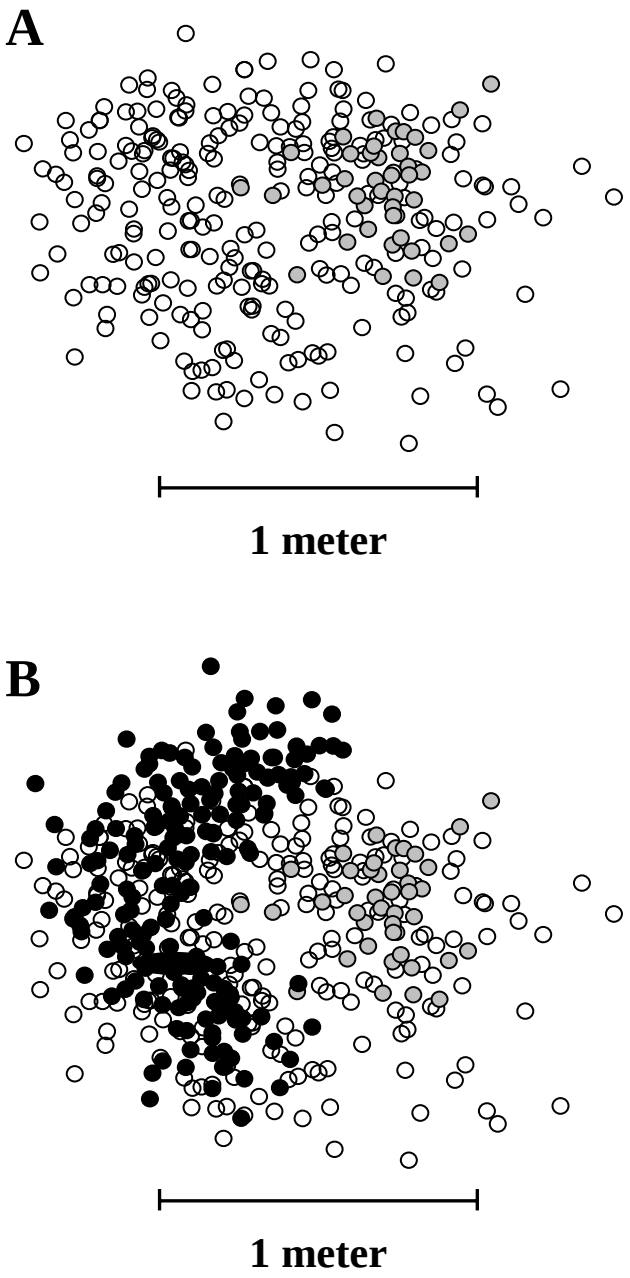

Figure 3.-An example of the spatial pattern of pre-spawning digging (A) made by chum salmon during redd construction. Gray circles represent the digs made in the hour immediately preceding spawning. The post-spawning covering dig pattern (B) is represented by the high density of black circles forming an arc immediately upstream of the egg deposition area.

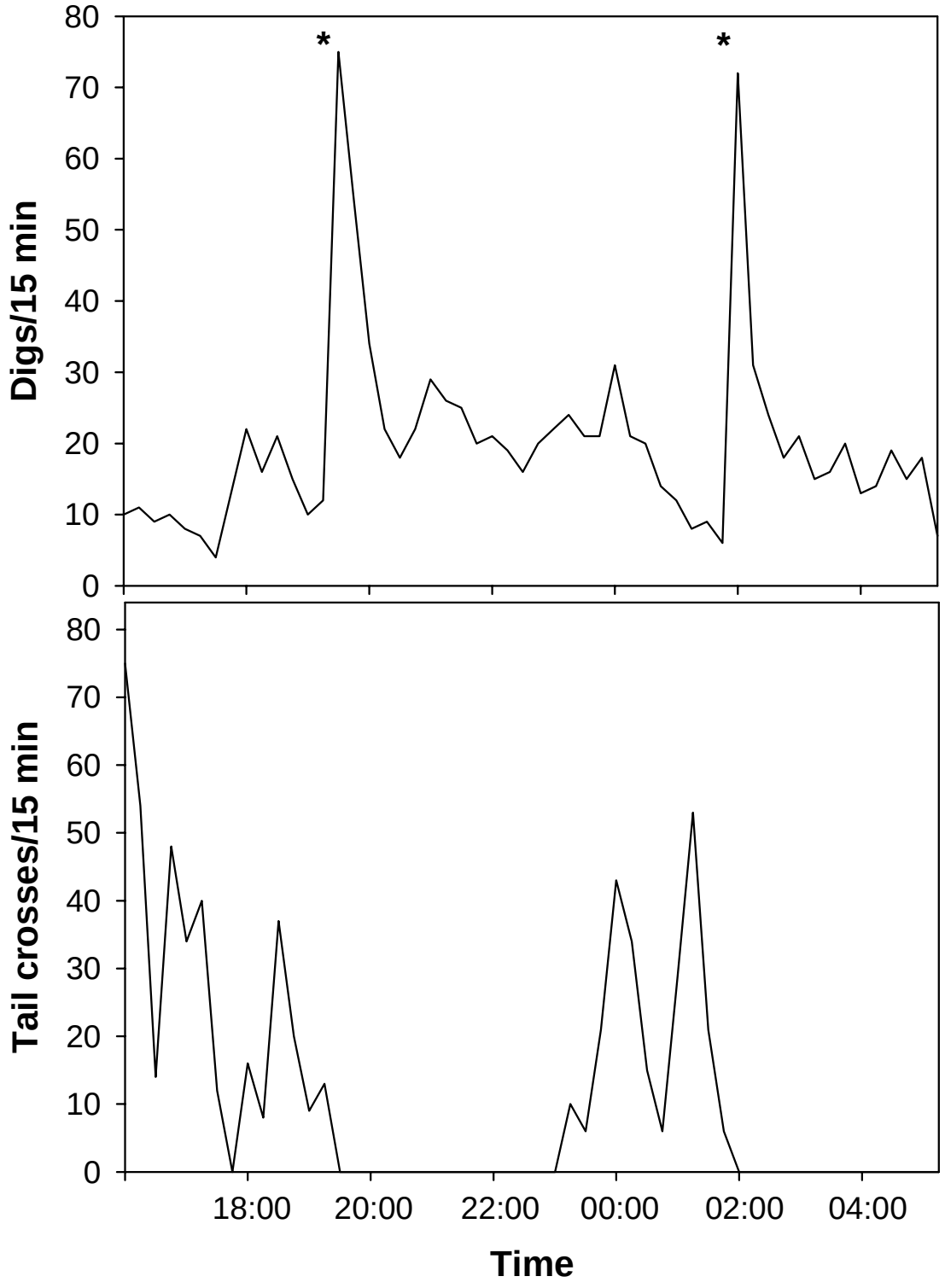

Figure 4.-The patterns of digging (top panel) and tail crossing (bottom panel) for a pair of spawning chum salmon observed for 14 h on November 19-20, 2003. Two spawning events were observed at 19:37 and 01:37 and are denoted with asterisks.

Table 1.-Summary of diel chum salmon spawning behaviors in 2003. Means, ranges, and standard deviations (SD) are for 15-min intervals. N=11 fish for which both daytime and nighttime data was collected. Two-sample *t*-test statistics and *P* values are shown for diel comparisons within each behavior. Values for the *t* statistic in the table were not significant at *P*=0.05.

Behavior	Diel period	Mean	Range	SD	*t*	*P* value
Digging	Day	7.7	2.9-11.8	3.12	0.19	0.8537
	Night	7.5	1.5-13.3	4.25		
Tail crossing	Day	14.1	0.6-75.0	21.66	0.33	0.7413
	Night	11.4	0-53.0	15.07		
Female chases	Day	0.23	0-0.5	0.17	0.36	0.7260
	Night	0.20	0-0.7	0.23		
Male chases	Day	0.53	0-1.2	0.47	-0.36	0.7224
	Night	0.62	0-2.6	0.76		

spawn with one female. Immediately after the spawning event, the male fish would reoccupy his position downstream of the female, or leave, while the female began covering the eggs.

Both female and male chum salmon were observed chasing other fish in defense of their nest during the day and the night. Chasing events were highly variable over time and were dependent on the number of other chum salmon in the area (Table 1). The courting males primarily chased other chum salmon. The females also chased conspecifics, but chased away smaller fish at night as well. These fish were likely peamouth *Mylocheilus caurinus* and northern pikeminnow *Ptychocheilus oregonensis* (U.S. Fish and Wildlife Service, unpublished data), and averaged 280 mm in length. These fish were only observed at night and were not abundant. Our statistical analyses found no diel differences in either male or female chasing behavior with the exception of a significant interaction between spawning incidence and diel period ($F = 5.83$, $P = 0.0274$) for male chases. This was due to a single male fish that engaged in a high number of chasing events during the night before eventual daytime spawning.

Discussion

Nighttime spawning by Pacific salmon is largely an undocumented phenomenon, which is likely due to the limitations and difficulties of collecting observational data in darkness without disturbing the fish. Past research has documented some aspects of nighttime spawning, but behavioral data was not collected. Berejikian et al. (2001) found that captively-reared Chinook salmon *Oncorhynchus tshawytscha* constructed redds at night in an experimental channel, but they did not determine if spawning occurred. Tautz and Groot (1975) used hydrophones to record the sound and frequency of digs made by chum salmon in an experimental channel to show that digging and spawning occurs during the day and night. More recently, McMichael et al. (2003) used hydrophones to record the nighttime acoustic digging signatures of spawning fall Chinook salmon below Wanapum Dam on the Columbia River. Although hydrophones can be used to document digging activity, observational data must be collected during the day to define the changes in digging frequency or signature that would indicate a spawning event. This approach also precludes the collection of additional behavioral information on spawning fish.

The DIDSON enabled us to describe various aspects of chum salmon spawning behavior at night that otherwise would not have been possible. Because the DIDSON uses sound to form images rather than light, we were able to obtain detailed images of spawning chum salmon in complete darkness without disturbing fish behavior. In addition, the planar view of images allowed us to identify changes in tail crossing behavior by courting males and the spatial pattern of digs made by females to document spawning events during the day and night. These criteria, in combination with changes in digging frequency, were essential for identifying spawning events because the release of gametes was not observable with the DIDSON. We found that immediately after spawning, the spatial pattern of digging changed, the frequency of digging increased rapidly, and tail crossing by the courting male ceased, which was consistent with the spawning event criteria described by Tautz and Groot (1975) and Schroder (1981) for chum salmon.

We documented nine nighttime and four daytime spawning events for chum salmon spawning below Bonneville Dam, and we did not find any significant differences in mean pre-spawning digging, tail crossing, and chasing events between the day and the night. It appears that once chum salmon begin nest construction and courtship, it continues until a spawning event occurs regardless of time of day. The entire process for a female chum salmon to dig 4-6 nests (Helle 1982) and deposit all her eggs may take 30-40 h (Tautz and Groot 1975; Schroder 1981). One reason for chum salmon engaging in continuous diel spawning activity may relate to the relatively short period of time fish have available on the spawning grounds before they die. The life expectancy of chum salmon at Ives Island once they reach the spawning ground is 7-10 d (Todd Hillson, Washington Department of Fish and Wildlife, personal communication). During that time, a female fish must claim a territory, construct multiple nests and spawn, and then defend her territory for as long as possible to preclude later-arriving fish from using her nests for spawning. This may be particularly critical at high spawner densities for which there may be increased competition for space (Schroder 1973). The density of chum salmon spawning in our study area can be quite high (6,694 fish in 2002 (van der Naald et al. 2003)), and we often observed eggs being excavated from the gravel during nest construction by later arriving females using underwater videography.

Chum salmon are capable of carrying out all aspects of spawning behavior in complete darkness in the apparent absence of visual cues with perhaps the exception of mate selection. The importance of body coloration to spawning Pacific salmon is well documented (see reviews in Groot and Margolis 1991), and the importance of body coloration and patterning as visual cues for mate selection in chum salmon has been well studied by Schroder (1981) and Duker (1982). Because the fish we selected for study were already engaged in nest construction and courtship behavior, we were unable to determine if chum salmon initially select spawning sites and mates differentially between the day and the night. We speculate that once spawning sites and mates are selected, visual cues become less important during the remainder of the spawning cycle allowing them to spawn at night as well as during the day.

Non-visual cues (i.e., tactile, auditory, olfactory) are likely the primary means by which chum salmon perceive other fish and their environment at night. Daytime video observation of male tail crossing behavior often showed the male making physical contact with the female fish, which may enhance the female's perception of this behavior at night. In addition, male quivering, which we observed during the day by underwater videography, may be detected by the female at night via the lateral line system. Both female and male fish may use this system to detect intruding fish as evidenced by chase events at night that were often initiated upon fish that were over 1 m away. Duker (1982) proposed a generalized model of the cues used in species recognition in Pacific salmon, but he did not discuss the possible role that the lateral line may play in detecting auditory cues. Duker predicted that male chum salmon that were experimentally blinded would not spawn in the absence of visual cues, but it is unclear whether this prediction was tested. It is possible that chum salmon can see to some extent in darkness that would at least permit recognition of body shape and form and enable them to spawn at night.

Our finding that chum salmon actively spawn at night has several implications for water management below Bonneville Dam on the Columbia River. Elevated nighttime flows may cause chum salmon habitat to become unsuitable for spawning. Garland et al. (2003) used a two-

dimensional hydrodynamic model and chum salmon spawning habitat criteria to predict changes in spawning habitat in our study areas over a range of flows. They found that at flows exceeding 3,965 m^3/s, the amount of suitable spawning habitat available for chum salmon was reduced in our study area, likely due to increased water velocities. During 2003, these flows were exceeded in our study area on 17 nights from November 1 to December 15—the primary chum salmon spawning period—however our observations did not coincide with these events. Under these flows, fish may have held position, moved into slower velocities near the shoreline, or left the area completely.

During periods of nighttime reverse load following at Bonneville Dam, the increase in water surface elevations at spawning sites may cause chum salmon to spawn at higher bed elevations that may become dewatered when flows subsequently decline. For this to occur, flows would need to be elevated for some period of time to allow the establishment of hyporheic upwelling that chum salmon use for locating their spawning nests (Geist et al. 2002). Additionally, chum salmon would need sufficient time to select a spawning site and construct a nest. In 2003, periods of high nighttime flows (> 4,248 m^3/s) lasted up to 11 h (U.S. Army Corps of Engineers 2003). It is unknown whether this is sufficient time to foster the physical habitat and behavioral conditions that would induce chum salmon to spawn at higher riverbed elevations under increased nighttime flows.

It is clear from this study that chum salmon do indeed spawn during nighttime hours, and therefore careful evaluations of reverse load following and its effects on chum spawning should continue to further inform hydrosystem management decisions that affect this population. Future investigations should quantify the effects of increased nighttime water elevations on chum salmon spawning behavior, location of redd formation, and the spatial and temporal distribution of redds in the Ives Island study area. Finally, findings should be integrated to evaluate options to shape Bonneville Dam discharges to optimize successful chum salmon spawning over a range of projected adult returns.

References

Belcher, E., B. Matsuyama, and G. Trimble. 2001. Object identification with acoustic lenses, pp. 6-11. Proceedings of Oceans 2001 Conference, 5-8 November, Honolulu, Hawaii.

Berejikian, B.A., E.P. Tezak, and S.L. Schroder. 2001. Reproductive behavior and breeding success of captively reared Chinook salmon. North American Journal of Fisheries Management 21:255-260.

Duker, G.J. 1982. Instream orientation and species recognition by Pacific salmon. Pages 286-295 *in* E.L. Brannon and E.O. Salo, editors. Salmon and trout migratory behavior symposium. University of Washington, Seattle, Washington.

Federal Energy Regulatory Commission. 1988. Vernita Bar Settlement Agreement. Docket No. E-9569-000. Federal Energy Regulatory Commission, Washington, D.C.

Fish Passage Center. 2003. System Operational Request #2003-15. Available: www.fpc.org/sors/2003-SOR/2003-15.pdf. (June, 2004).

Garland, R.D., K.F. Tiffan, D.W. Rondorf, J.J. Skalicky, and D.A. Anglin. 2003. Assessment of fall chinook and chum salmon spawning habitat near Ives and Pierce islands in the Columbia River. Report to the Bonneville Power Administration, Contract 00004701, Portland, Oregon.

Geist, D.R., T.P. Hanrahan, E.V. Arntzen, G.A. McMichael, C.J. Murray, and Y. Chien. 2002. Physicochemical characteristics of the hyporheic zone affect redd site selection by chum salmon and fall Chinook salmon in the Columbia River. North American Journal of Fisheries Management 22:1077-1085.

Groot, C., and L. Margolis, editors. 1991. Pacific salmon life histories. University of British Columbia Press, Vancouver.

Helle, J.H. 1981. Significance of the stock concept in artificial propagation of salmonids in Alaska. Canadian Journal of Fisheries and Aquatic Sciences 38:1665-1671.

Hymer, J. 1997. Results of studies on Chinook spawning in the mainstem Columbia River below Bonneville Dam. Columbia River Progress Report 97-9. Washington Department of Fish and Wildlife, Battleground, Washington.

Johnson, O.W., W.S. Grant, R.G. Kope, K. Neely, F.W. Waknitz, and R.S. Waples. 1997. Status review of chum salmon from Washington, Oregon, and California. NOAA Technical Memorandom NMFS-NWFSC-32, Seattle, Washington.

McMichael, G.A., C.A. McKinstry, and J.A. Carter. 2003. Fall Chinook salmon spawning activity versus daylight and flow below Wanapum Dam. Pages 4.2-1 to 4.2-14 *in*

Chinook Salmon in the Priest Rapids Project. Report to Grant County Public Utility District, No. 2, Contract 430-794, Ephrata, Washington.

Moursund, R.A., T.J. Carlson, and R.D. Peters. 2003. A fisheries application of a dual-frequency identification sonar acoustic camera. ICES Journal of Marine Science 60:678-683.

National Marine Fisheries Service. 1999. Endangered and threatened species: threatened status of two ESUs of chum salmon in Washington and Oregon. Federal Register 64:14508-14517.

SAS Institute Inc. 2000. SAS/STAT users guide, release 8.1. SAS Institute Inc., Cary, North Carolina.

Schroder, S.L. 1973. Effects of density on the spawning success of chum salmon (Oncorhynchus keta) in an artificial spawning channel. Master's thesis, University of Washington, Seattle.

Schroder, S.L. 1981. The role of sexual selection in determining overall mating patterns and mate choice in chum salmon. Doctoral dissertation, University of Washington, Seattle.

Tautz, A.F., and C. Groot. 1975. Spawning behavior of chum salmon (*Oncorhynchus keta*) and rainbow trout (*Salmo gairdneri*). Journal of the Fisheries Research Board of Canada 32:633-642.

Tiffan, K.F., D.W. Rondorf, and J.J. Skalicky. In press. Imaging fall Chinook salmon redds in the Columbia River with a dual-frequency identification sonar. North American Journal of Fisheries Management.

U.S. Army Corps of Engineers. 2003. Bonneville Dam and Lake on Columbia River, Outflow discharge. Available: www.nwd-wc.usace.army.mil/cgi-bin/dataquery.pl?k=columbia+river+flow. (June, 2004).

van der Naald, W., R. Clark, R. Brooks, and C. Duff. 2003. Evaluation of fall Chinook and chum salmon spawning below Bonneville Dam. Annual Report to the Bonneville Power Administration, contract 99BI15006/99BI15007, Portland, Oregon.